

WARM CLIMATES IN EARTH HISTORY

EDITED BY

BRIAN T. HUBER, *Smithsonian Institution*

KENNETH G. MACLEOD, *University of Missouri*

SCOTT L. WING, *Smithsonian Institution*

 **CAMBRIDGE**
UNIVERSITY PRESS

PUBLISHED BY THE PRESS SYNDICATE OF THE UNIVERSITY OF CAMBRIDGE
The Pitt Building, Trumpington Street, Cambridge, United Kingdom

CAMBRIDGE UNIVERSITY PRESS
The Edinburgh Building, Cambridge CB2 2RU, UK www.cup.cam.ac.uk
40 West 20th Street, New York, NY 10011-4211, USA www.cup.org
10 Stamford Road, Oakleigh, Melbourne 3166, Australia
Ruiz de Alarcón 13, 28014 Madrid, Spain

© Cambridge University Press 2000

This book is in copyright. Subject to statutory exception
and to the provisions of relevant collective licensing agreements,
no reproduction of any part may take place without
the written permission of Cambridge University Press.

First published 2000

Printed in the United Kingdom at the University Press, Cambridge

Typeset in Times

A catalogue record for this book is available from the British Library

Library of Congress Cataloguing in Publication data

Warm climates in earth history / edited by Brian T. Huber, Kenneth G.
MacLeod, and Scott L. Wing.

p. cm.

Includes index

ISBN 0 521 64142 X hardback

1. Paleoclimatology. 2. Earth sciences. I. Huber, Brian T.
II. MacLeod, Kenneth G., 1964- . III. Wing, Scott L.

QC884.W37 1999

551.6'09'01-dc21 98-51724 CIP

ISBN 0 521 64142 X hardback

An early Eocene cool period? Evidence for continental cooling during the warmest part of the Cenozoic

SCOTT L. WING, HUIMING BAO, AND PAUL L. KOCH

ABSTRACT

During the late Paleocene global temperatures began to rise toward their Cenozoic acme, which was reached during the early Eocene. Most detailed studies of temperature change during the Paleocene–Eocene time interval have been based on isotopic analyses of microfossils from marine sections. For this study we estimated changes in paleotemperature for continental environments in the Bighorn Basin, Wyoming, based on leaf margin analyses of fossil floras. The leaf margin analyses show that over the last 2 million years of the Paleocene mean annual temperature increased from $12.9(\pm 2.4)$ to over $15(\pm 2.4)$ °C, but that during the first million years of the Eocene temperatures dropped from $18.2(\pm 2.3)$ to $10.8(\pm 3.3)$ °C. The strong temperature decline was followed by a rapid increase to $15.8(\pm 2.2)$ °C then $22.2(\pm 2.0)$ °C in the lower part of Chron 24n. The absence of megaflores during the short Late Paleocene Thermal Maximum (LPTM) prevented us from making temperature estimates based on leaf margin analysis. Early Eocene cooling is corroborated through oxygen isotope analysis of authigenic minerals in paleosols. These minerals record changes in the $\delta^{18}\text{O}$ value of surface water, which may be related to changes in temperature and vapor transport to the region. The $\delta^{18}\text{O}$ value of surface water dropped 4‰ during the early part of the early Eocene, consistent in direction and magnitude with the cooling inferred from the flora. The $\delta^{18}\text{O}$ values of soil carbonates from the LPTM increase by ~ 1 ‰, consistent with warming above background Paleocene temperatures by ~ 4 °C. Few previous studies of this globally warm time interval have noted cooling during the early Eocene. Here we briefly summarize faunal and floral turnover during the Paleocene–Eocene transition and explore the implications of early Eocene cooling for climatic and biotic change.

INTRODUCTION

It is clear from geological and paleontological evidence that warm middle and high latitudes were the typical climatic state for the earth during most of the Phanerozoic. The most extreme and extended warm intervals in earth history occurred in the Mesozoic and Paleozoic, distant enough in the past so that the continental positions are arguable, few isotopic temperature estimates are available,

fine resolution of geological time is difficult, and biotas are highly dissimilar to living faunas and floras. All of these factors make the climates of these remote times difficult to characterize both geographically and in terms of shorter-term fluctuations.

The early Cenozoic, especially early Eocene, is increasingly being recognized as a key period for understanding the climate and biogeography of globally warm intervals of earth history. The early Cenozoic is recent enough that continental configurations are not radically different from the present, fossils and sediments are widely distributed and amenable to relatively precise radiometric and paleomagnetic dating, and the organisms present can be understood relatively well by comparing them with the living biota. The early Eocene is a kind of outpost of warm Mesozoic climate surviving to within 50 million years of the present.

The pattern of temperature change during the late Paleocene and early Eocene has been defined largely through measurements of stable oxygen isotopes in foraminiferal tests taken from ocean floor drill cores (e.g., Miller *et al.*, 1987; Zachos *et al.*, 1994). Although individual records vary, the overall trend is that ocean waters warmed substantially during the last half of the Paleocene and the first 2–3 million years of the Eocene. Oxygen isotopic analyses of benthic foraminifera indicate that deep-sea temperatures warmed from 7–10°C in the late Paleocene to 10–14°C in the early Eocene; analyses of planktic foraminifera indicate that middle- to high-latitude sea-surface temperatures increased from 11–20°C in the late Paleocene to 14–24°C in the early Eocene (Zachos *et al.*, 1994). During this strong middle- and high-latitude warming, tropical sea-surface temperatures apparently remained nearly constant in the 20–26°C range (Schrag *et al.*, 1992; Zachos *et al.*, 1994). Warming around the Paleocene–Eocene transition appears to be largely a middle- and high-latitude phenomenon.

Middle- to high-latitude continental climates also appear to have warmed from the late Paleocene to the early Eocene. Terrestrial floras from southeastern coastal Alaska indicate a warmer climate during deposition of the early Eocene Tolstoi Formation than the late Paleocene Chickaloon Formation (Wolfe, 1966, 1972, 1977), and floristic evidence for warming has been noted in North Dakota and Wyoming (Leopold and MacGinitie, 1972; Hickey, 1977). The increasing species diversity and size range of ectothermic vertebrates also indicate warming from the Paleocene to the Eocene in the interior of western North America (Hutchison 1982; Markwick, 1994). Previous paleotemperature estimates based on floras from the Bighorn and Wind River basins in Wyoming show that mean annual temperature increased from 13 to 21°C during the late Paleocene and early Eocene (Hickey, 1980; Wing *et al.*, 1991). The early Eocene has also been noted as a time of exceptional warmth in East Asia (Guo, 1985), Siberia (Budantsev, 1992), Australia (Christophel and Greenwood, 1989), western Europe (Collinson and Hooker, 1987), and southern South America (Romero, 1986). Low-latitude floral data for this time are scarce, but the floristic composition of Eocene floras from Panama is consistent with low-latitude temperatures in the modern range (Graham, 1992).

High-resolution studies of the Paleocene–Eocene boundary interval have revealed a short period of intense middle- and high-latitude warmth in the latest

Paleocene, commonly referred to as the Late Paleocene Thermal Maximum, or LPTM (Kennett and Stott, 1991; Zachos *et al.*, 1994; Corfield and Norris, 1996). During this ~ 100 ka interval, isotopic temperature estimates for high-latitude ocean waters suggest an $\sim 5^\circ\text{C}$ increase in sea-surface temperature and near elimination of vertical temperature gradients in high-latitude oceans. A coeval increase in kaolinite in nearshore marine sediments indicates more rapid chemical weathering and enhanced runoff from continental surfaces at middle and high latitudes (Gibson *et al.*, 1993; Robert and Kennett, 1994). Several major biotic turnover events also took place during the LPTM, including a major immigration of new mammalian lineages in North America; this immigration event marks the beginning of the Wasatchian land mammal age, and the distinctive earliest Wasatchian assemblage has been called the Wa0 fauna (Gingerich, 1989). The LPTM also coincides with a $\sim 4\text{‰}$ negative excursion in carbon isotopes that has been observed in both marine and continental sections (e.g., Kennett and Stott, 1991; Koch *et al.*, 1992). This isotopic marker has been used to establish the synchronicity of biotic and climatic events in the oceans and on the continents during the LPTM (e.g., Koch *et al.*, 1995). The cause of the carbon isotope excursion and LPTM is debated, but may relate to the release of large quantities of methane over a period of ~ 10 ka that resulted from the dissociation of sea-floor clathrates (Dickens *et al.*, 1997).

In this paper we present a high-resolution record of temperature across the Paleocene–Eocene boundary interval in the Bighorn Basin of northern Wyoming, based on a combination of leaf margin data and oxygen isotope data from hematite and calcite in paleosols. Our data show the expected warming across the Paleocene–Eocene interval, but also an interval of strong cooling during the early Eocene that lasted ~ 1 million years. Scattered data from other areas suggest that this cooling was at least continental to hemispheric in scale rather than strictly local. We also briefly compare the record of biotic changes in the Bighorn Basin with the record of temperature change, and find evidence that diversity and composition of floras and faunas were affected by the cooling. This phenomenon will have to be accounted for in models of climatic change during the early Cenozoic and in considering the biotic consequences of climatic change.

GEOLOGICAL CONTEXT

Lithostratigraphy

The Paleocene–Eocene transition in the Bighorn Basin is recorded by rocks of the upper Fort Union and lower Willwood formations (Bown, 1980; Rose, 1981; Wing and Bown, 1985). Stratigraphic sections have been measured across the Paleocene–Eocene interval in seven areas of the Bighorn Basin: North Butte, Worland East, Sand Creek Divide, Gould Butte, Antelope Creek/Elk Creek, Foster Gulch/McCullough Peaks, and Polecat Bench/Clarks Fork Basin (Fig. 7.1; Bown, 1979; Gingerich *et al.*, 1980; Schankler, 1980; Clyde *et al.*, 1994; Bown *et al.*, 1994a; Wing, 1998). Areas of exposed Paleogene rocks are separated from one another by areas of Quaternary alluvium, so that correlations among them are generally made through mammalian biostratigraphy, magnetostratigraphy, and

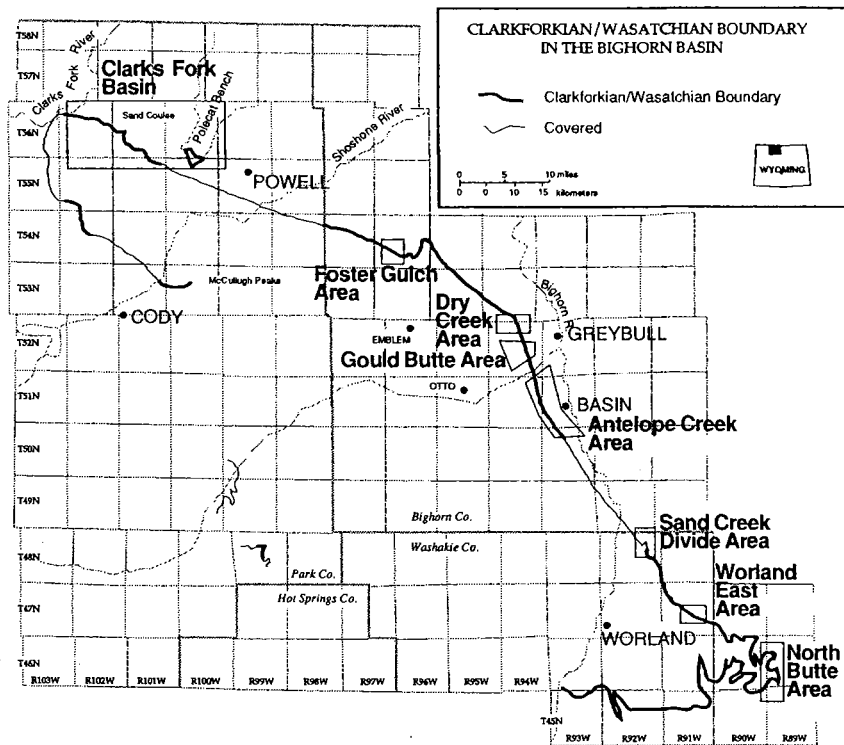


Figure 7.1. Map of the Bighorn Basin showing major field areas for the Paleocene–Eocene boundary interval.

carbon isotope values (Schankler, 1980; Gingerich, 1989; Clyde *et al.*, 1994; Tauxe *et al.*, 1994; Koch *et al.*, 1995). Within each field area local stratigraphic sections have been correlated by bed tracing and combined into composite sections that indicate the relative stratigraphic levels of hundreds of fossil localities. In all of the areas described in this work the sedimentary sequence across the Paleocene–Eocene transition lacks noticeable unconformities.

The dominant lithology in both the Fort Union and Willwood formations is mudstone, with variable lesser amounts of lenticular and sheet sandstones, carbonaceous shales, and in the Fort Union Formation, coal (Bown, 1980). Mudstones of the Willwood Formation are generally red or variegated in color, reflecting oxidation of iron compounds during pedogenesis in seasonally dry floodplain soils (Bown and Kraus, 1981a). Fort Union Formation mudstones are usually drab in color and higher in organic carbon content, and they probably represent wetter floodplain soils. The transition from drab Fort Union Formation mudstones to variegated Willwood Formation mudstones is coincident with the terminal Paleocene carbon isotope excursion and mammalian faunal change (the Clarkforkian/Wasatchian boundary) in many parts of the Bighorn Basin. However, in the Clarks Fork Basin the carbon isotope excursion and the beginning of the Wasatchian are more

than 350 m above the beginning of Willwood deposition (Rose, 1981), whereas in the Gould Butte area the lowest Wasatchian faunas occur at least 100 m below the lowest Willwood Formation (Wing and Bown, 1985). This diachroneity strongly suggests that soil-forming conditions on the floodplains were influenced by local subsidence or tectonism as well as by regional and global climate change (Wing and Bown, 1985). Within the Willwood Formation, carbonaceous shales alternate with oxidized mudstones on a stratigraphic scale of tens of meters. Lithological variation at this scale may be the result of autogenic fluvial processes, but could also be influenced by high-frequency climatic change such as Milankovitch cyclicity (Kraus and Aslan, 1993).

Chronology of the Paleocene–Eocene boundary interval

The chronology of the Paleocene–Eocene transition has been reviewed extensively in recent publications (e.g., Berggren *et al.*, 1995; Berggren and Aubry, 1996). Discussion here is limited to points that directly influence our age estimates for the Bighorn Basin. The two central problems that affect the calculation of ages in the Bighorn Basin are the calibration of the Geomagnetic Polarity Time Scale (GMPTS) of Cande and Kent (1992, 1995), and the calculation of an age for the carbon isotope excursion.

Cande and Kent (1992, 1995) used an age of 55 Ma for the Paleocene–Eocene boundary as one of the calibration points for their GMPTS. This age estimate was derived in the following fashion. The –17 ash in the North Sea, which has been dated at 54.5 Ma by Swisher and Knox (1991), occurs at 400 mbsf at Deep Sea Drilling Project (DSDP) Site 550. This level is 8 m above the NP9/NP10 boundary in the same hole (Aubry *et al.*, 1996). The NP9/NP10 boundary, which was about two-thirds of the way down from the top of C24r, was taken as an approximation of the Paleocene–Eocene boundary, and this position (C24r.66) was assigned an age of 55 Ma. The adjacent calibration points for the GMPTS used by Cande and Kent (1992, 1995) were 65 Ma for the K/T boundary (C29r.3), and 46.8 Ma for C21n.33. The ages of reversals between these calibration points were interpolated by scaling the widths of the corresponding sea-floor magnetic stripes to time using a spline function forced through the calibration points. Errors in dating the calibration points would cause the ages of surrounding reversals to be wrong as well.

In the last few years many aspects of the Paleocene–Eocene record at DSDP 550 have been reinterpreted. The transition from C24r to C25n may lie several meters lower than originally thought (Ali and Hailwood, 1998); this would have made the –17 ash and the NP9/NP10 boundary appear to be too near the bottom of C24r in the original interpretation. Sediment accumulation rates may not have been constant at DSDP 550. Specifically, Aubry *et al.* (1996) suggested that there might be significant hiatuses and dissolution intervals in the lower part of C24r. If these hiatuses represent a substantial interval of non-deposition or erosion they too would make the –17 ash appear to be nearer the bottom of C24r than it really is. These problems suggest that 55 Ma may be closer to the middle of C24r than to a position two-thirds of the way down in C24r, as assumed by Cande and Kent (1992,

Table 7.1. Calibration points for Bighorn Basin sections

Calibration point	Section*	Meter level	Age model 1	Age model 2	References for age and stratigraphic level
Top Chron 24n.2n	MPS	1400	52.757	52.907	Clyde <i>et al.</i> , 1994; Cande and Kent, 1995
Bentonitic tuff (^{40}Ar , ^{39}Ar)	ECS	634	52.8±0.3	52.8±0.3	Wing <i>et al.</i> , 1991
Top Chron 24n.3n	MPS	1300	52.903	53.072	Clyde <i>et al.</i> , 1994; Cande and Kent, 1995
Base Chron 24n.3n	MPS	950	53.347	53.566	Clyde <i>et al.</i> , 1994; Cande and Kent, 1995
Carbon isotope excursion	MPS	0	54.955	55.234	Koch <i>et al.</i> , 1995; this paper
Carbon isotope excursion	HCS	0	54.955	55.234	Koch <i>et al.</i> , 1995; this paper
Carbon isotope excursion	WES	0	54.995	55.234	Koch <i>et al.</i> , 1995; this paper
Carbon isotope excursion	CFB	1520	54.995	55.234	Koch <i>et al.</i> , 1995; this paper
Top of 25n	CFB	1070	55.904	56.215	Butler <i>et al.</i> , 1981; Cande and Kent, 1995
Base Chron 25n	CFB	820	56.391	56.688	Butler <i>et al.</i> , 1981; Cande and Kent, 1995
Top Chron 26n	CFB	500	57.554	57.791	Butler <i>et al.</i> , 1981; Cande and Kent, 1995

*CFB, Polecat Bench/Clarks Fork Basin composite section; ECS, Antelope Creek/Eik Creek composite section; HCS, Honeycombs section; MPS, Foster Gulch/McCullough Peaks composite section; WES, Worland East section. Models 1 and 2 are explained in the text.

1995). If this is true, then reversals in this part of the GMPTS are up to 300 ka older than indicated in the timescale of Cande and Kent (1995).

A second problem in the chronology of the Paleocene–Eocene boundary interval is the age of the carbon isotope excursion and its relative position within C24r. Aubry *et al.* (1996) argued that all of the DSDP sections being studied for Paleocene–Eocene boundary questions have long hiatuses within C24r, and that these hiatuses cause the carbon isotope excursion to appear stratigraphically higher within C24r than would be expected based on its temporal position near the base of the chron. It has also been postulated that there may be more than one carbon isotope excursion within C24r (Aubry *et al.*, 1996), although multiple excursions have not been demonstrated in any single section.

Berggren *et al.* (1995) and Aubry *et al.* (1996) estimated an age of 55.5 Ma for the carbon isotope excursion based in part on its position 1 m below the NP9/NP10 boundary and 9 m below the –17 ash at DSDP 550. They argued that much of the million years between the ash and the isotopic excursion was represented in this core by a hiatus at the NP9/NP10 boundary. There remains, however, substantial uncertainty in these interpretations. Aubry *et al.* (1996, p. 367) stated: ‘We emphasize that the temporal framework used here is highly speculative because our reconstruction is based on the unverifiable assumption that the sedimentation rates were essentially the same at Sites 550 and 690.’ There is no direct evidence for the length of the proposed NP9/NP10 hiatus at DSDP 550, and therefore we are only willing to conclude that the time between the excursion and the –17 ash must have been sufficient for the deposition of the 9 m of sediment between them at Site 550. At typical deep-sea sedimentation rates of 1–3 cm ka⁻¹, the 9 m should represent 300–900 ka, which gives a range of minimum ages for the carbon isotope excursion of 54.8–55.4 Ma. This minimum estimate is consistent with the 55.5 Ma estimate made by Aubry *et al.* (1996), but ages as young as 54.8 Ma are equally possible. We also point out that if much of the time between the carbon isotope excursion and the –17 ash is represented by a hiatus at Site 550 (Aubry *et al.*, 1996), this requires high rates of sedimentation above the NP9/NP10 boundary.

Age estimates for the Bighorn Basin

In order to place the temperature and isotopic records from the Bighorn Basin in a global context, we have calculated age estimates by linear interpolation between tie points of known or estimated age. These tie points include six magnetic polarity reversals, one radiometrically dated tuff and the carbon isotope excursion (Table 7.1). We have developed two age models for the stratigraphic levels within the three major composite sections: the Foster Gulch/McCullough Peaks section, the Antelope Creek/Elk Creek section, and the Polecat Bench/Clarks Fork Basin section (Tables 7.2–7.4). Age model 1 uses the ages for the GMPTS published by Cande and Kent (1992, 1995). Age model 2 relies on recalculated ages for the relevant polarity reversals. This recalculation has been done by removing the 55 Ma calibration point at C24r.33, and replacing it with a calibration point of 52.8 ± 0.3 Ma at the base of 24n.1n based on magnetic stratigraphy and a radiometric date in the Antelope Creek/Elk Creek section in the Bighorn Basin (Wing *et al.*, 1991; Tauxe *et al.*,

Table 7.2. Age calibration (in Ma) of Foster Gulch/McCullough Peaks Section

Meter level	Age model 1	Age model 2	Sample/Event
1420	-52.728	-52.874	<i>Lambdaotherium</i> FAD
1400	-52.757	-52.907	Top 24n.2n
1300	-52.903	-53.072	Top 24n.3n
1100	-53.157	-53.354	<i>Heptodon</i> FAD
950	-53.347	-53.566	Base 24n.3n
880	-53.436	-53.665	<i>Bunophorus</i> FAD
0	-54.955	-55.234	Wa0 - carbon isotope excursion
	0.685	0.561	Accumulation rate 0-880 m (m ka ⁻¹)
	0.788	0.709	Accumulation rate 880-1300 m (m ka ⁻¹)
	0.579	0.606	Accumulation rate 1300-1400 m (m ka ⁻¹)

Bold numbers are calibration points (age fixed); models 1 and 2 are explained in the text.

1994). Ages of the magnetic reversals were recalculated by linear interpolation (Table 7.5). Age model 2 does not rely on any marine calibration points in the late Paleocene or early Eocene.

Although the age estimates for the paleomagnetic reversals and the tuff are straightforward, the age estimate for the carbon isotope excursion requires explanation. Given the difficulties described above in using deep-sea marine sections to derive an age model for events during C24r, we do not accept the most recent published age estimate of 55.5 Ma for the carbon isotope excursion (Aubry *et al.*, 1996, Berggren and Aubry, 1996). Instead we calculate the age of the carbon isotope excursion based on its stratigraphic position within the Polecat Bench/Clarks Fork Basin section, where there is no evidence for lengthy hiatuses or large shifts in depositional rates within C24r. This requires a three-step process because there is no single Bighorn Basin section in which both the top and the bottom of C24r have been identified, and therefore there is no direct way to establish the relative position of the carbon isotope excursion within C24r. The first step is to estimate the age of the first appearance of the mammal *Bunophorus*, which is known from all three composite sections in the Bighorn Basin. This is done in the Foster Gulch/McCullough Peaks section, which we chose because of the stable magnetic behavior of the sediments there (Clyde *et al.*, 1994). The top and base of C24n.3 occur at 1300 and 950 m, respectively, in this section (Table 7.2; Clyde *et al.*, 1994). The ages for these magnetic boundaries are used to calculate the sedimentation rate, and this rate is extrapolated to the 880 m level to estimate the age of the First Appearance Datum (FAD) of *Bunophorus* in this section (53.436 Ma in model 1, 53.665 in model 2). In the second step the age for the FAD of *Bunophorus* is assigned to the 2240 m level of the Polecat Bench/Clarks Fork Basin section, the level of its FAD in this section (Gingerich, 1991). Finally, the age of the carbon isotope excursion (1520 m [Koch *et al.*, 1992]) is estimated by linear interpolation between the FAD of *Bunophorus* at

Table 7.3. Age calibration (in Ma) of Elk Creek section

Meter level	Age model 1	Age model 2	Sample/Event
634	-52.800	-52.800	³⁹ Ar/ ⁴⁰ Ar date
621	-52.831	-52.842	LMA-8
601	-52.878	-52.906	HOA-YPM33
591	-52.902	-52.938	<i>Lamdotherium</i> FAD
571	-52.949	-53.002	HOA-YPM1
546	-53.008	-53.083	HOA-D1467
485	-53.152	-53.279	HOA-D1531
468	-53.192	-53.334	LMA-7 top
438	-53.263	-53.456	HOA-D1398
430	-53.282	-53.430	<i>Heptodon</i> FAD
420	-53.306	-53.488	LMA-7 bottom
409	-53.332	-53.523	HOA-D1454
380	-53.400	-53.616	Biohorizon B
378	-53.405	-53.623	HOA-D1300
378	-53.405	-53.623	HOA-D1301
365	-53.436	-53.665	<i>Bunophorus</i> FAD (from MPS)
353	-53.486	-53.716	LMA-6 top
336	-53.556	-53.789	HOA-D1374
311	-53.661	-53.897	LMA-6 bottom
290	-53.748	-53.987	HOA-YPM350R
290	-53.748	-53.987	HOA-YPM350
210	-54.081	-54.331	HOA-YPM290
200	-54.122	-54.374	LMA-5 top
190	-54.164	-54.417	Biohorizon A
140	-54.372	-54.632	HOA-YPM104
110	-54.497	-54.761	LMA-5 bottom
105	-54.518	-54.783	LMA-4 top
100	-54.539	-54.804	HOA-YPM119
38	-54.797	-55.071	FAD <i>Platycarya</i> pollen
30	-54.830	-55.105	HOA-YPM115
10	-54.913	-55.191	LMA-4 bottom
0	-54.955	-55.234	Wa0 red beds (lithology only)
-7	-54.984	-55.264	LMA-3 top
-67	-55.234	-55.522	LMA-3 bottom
-172	-55.670	-55.974	LMA-2 bottom
-305	-56.224	-56.546	LMA-1 bottom
	0.240	0.233	Accumulation rate 0-365 m (m ka ⁻¹)
	0.423	0.311	Accumulation rate 365-634 m (m ka ⁻¹)

Bold numbers are calibration points (age fixed); models 1 and 2 are explained in the text.

2240 m and the bottom of C24r at 1070 m (Table 7.4; Butler *et al.*, 1981). Note that regardless of the age model, the carbon isotope excursion is likely to be only slightly less than two-thirds (63%) of the way down from the top of C24r, because the FAD of *Bunophorus* is only slightly older than the top of C24r. This stratigraphic position relative to the top and bottom of C24r is roughly the same one seen in DSDP Sites

Table 7.4. Age calibration (in Ma) of Polecat Bench/Clarks Fork Basin Section

Meter level	Age model 1	Age model 2	Sample/Event
2240	-53.436	-53.665	<i>Bunophorus</i> FAD date from MRS
1895	-54.164	-54.417	HOA-SC232
1860	-54.237	-54.493	Biohorizon A
1850	-54.259	-54.515	HOA-SC34
1780	-54.406	-54.667	HOA-SC313
1720	-54.533	-54.798	HOA-SC12
1620	-54.744	-55.016	HOA-SC18
1570	-54.849	-55.125	HOA-SC4
1570	-54.849	-55.125	HOA-SC123
1535	-54.923	-55.201	HOA-SC40
1520	-54.955	-55.234	Wa0 - carbon isotope excursion
1500	-54.997	-55.278	HOA-SC138
1455	-55.092	-55.376	HOA-SC90
1455	-55.092	-55.376	HOA-SC90R
1400	-55.208	-55.496	Youngest Cf2/Cf3
1355	-55.303	-55.594	HOA-SC127
1310	-55.398	-55.692	Oldest Cf2/Cf3
1250	-55.524	-55.823	LMA-2 midpoint
1210	-55.609	-55.910	HOA-SC92
1160	-55.714	-56.019	Tfu/Tw contact
1160	-55.714	-55.019	Cf1/Cf2
1090	-55.862	-56.171	HOA-SC171
1070	-55.904	-56.215	Top of 25n
1000	-56.040	-56.347	LMA-1 midpoint
950	-56.138	-56.442	Youngest base for Clarkforkian
850	-56.333	-56.631	Oldest base for Clarkforkian
820	-56.391	-56.688	Base of 25n
500	-57.554	-57.791	Top of 26n
	0.275	0.290	Accumulation rate 500-820 m ($m ka^{-1}$)
	0.513	0.529	Accumulation rate 820-1070 m ($m ka^{-1}$)
	0.474	0.459	Accumulation rate 1070-1520 m ($m ka^{-1}$)

Bold numbers are calibration points (age fixed); models 1 and 2 explained in the text.

549 and 550. Age model 1 estimates the carbon isotope excursion to be at 54.995 Ma; model 2 yields an estimate of 55.234 Ma (Tables 7.1 and 7.4). These age estimates are within the range anticipated for the carbon isotope excursion based on DSDP 550 (see discussion above).

The age calibration of stratigraphic levels for each of the three major composite sections is shown in Tables 7.2-7.4. Below we briefly discuss the positions and correlation of the tie points in each section.

The lower three paleomagnetic tie points, the top of C26n, and the base and top of C25n, have been observed in the Clarks Fork Basin section along Polecat Bench (Butler *et al.*, 1981), where they occur in rocks that produce late Tiffanian or Clarkforkian mammals. Clarkforkian faunas in the eastern and southeastern

Table 7.5. *Recalibration of magnetic reversals*

Reversal	Cande and Kent (1995)	This paper (model 2)	Difference
C21n (0.33)	46.800	46.800	0.000
Top C22n	49.037	49.252	0.215
Base C22n	49.714	49.958	0.244
Top C23n.1n	50.778	51.028	0.250
Base C23n.1n	50.946	51.192	0.246
Top C23n.2n	51.047	51.291	0.244
Base C23n.2n	51.743	51.955	0.212
Top C24n.1n	52.364	52.529	0.165
Base C24n.1n	52.663	52.800	0.137
Top C24n.2n	52.757	52.907	0.150
Base C24n.2n	52.801	52.956	0.155
Top C24n.3n	52.903	53.072	0.169
Base C24n.3n	53.347	53.566	0.219
C24r (0.66)	55.000	55.315	0.315
Top C25n	55.904	56.215	0.311
Base C25n	56.391	56.688	0.297
Top C26n	57.554	57.791	0.237
Base C26n	57.911	58.125	0.214
Top C27n	60.920	60.903	-0.017
Base C27n	61.276	61.234	-0.042
Top C28n	62.499	62.385	-0.114
Base C28n	63.634	63.486	-0.148
Top C29n	63.976	63.827	-0.149
Base C29n	64.745	64.614	-0.131
C29r (0.3)	65.000	65.000	0.000

Bold numbers are age calibration points.

Bighorn Basin are very poorly known, and paleomagnetic analysis has not been done in the Fort Union Formation in this area, making correlation to the northern Bighorn Basin difficult

The carbon isotope excursion has been observed in the Clarks Fork Basin, Foster Gulch, Sand Point Divide, Worland East, and North Butte areas, outcropping over a distance of ~130 km (Koch *et al.*, 1992, 1995). In all regions, the negative carbon isotope values come from distinctive, thick, red paleosols that also produce the basal Wasatchian (Wa0) mammalian fauna first noted by Gingerich (1989). The Wa0 fauna has been collected from the thick red beds in one additional area on the west side of the basin (Hole-in-the-Ground), but this region has not been sampled for carbon isotopes. In the Antelope Creek/Elk Creek area in the eastern Bighorn Basin there are distinctive, thick, red beds at the base of the Willwood Formation that appear to correspond to the Wa0 red beds, but mammalian fossils and nodules suitable for stable carbon isotope analysis have not been found. Besides their stratigraphic position at the base of the Willwood Formation, there are three other reasons to think that the basal red beds on Antelope Creek represent the carbon isotope excursion and Wa0 interval. Firstly, early Wasatchian faunas (Wa1 or lower

Haplomylus–*Ectocion* zone) are known from a level 50 m above the basal red beds (Schankler, 1980). Secondly, late Paleocene palynomorphs and megafossils occur in Fort Union rocks less than 50 m beneath the basal red beds (Wing, 1984). Thirdly, the first occurrence of *Platycarya* pollen is 38 m above the basal red bed in this section (G. Harrington, personal communication, 1997; *contra* Wing *et al.*, 1991). In eastern North America the *Platycarya* FAD is in the uppermost decimeters of NP9 (Frederiksen, 1979, 1980), and the NP9/NP10 boundary occurs above the carbon isotope excursion, but within C24r (Gibson *et al.*, 1993). The inference that the thick red beds at the base of the Antelope Creek/Elk Creek section contain the carbon isotope excursion, as they do elsewhere in the basin, is consistent with the occurrence of the carbon isotope excursion within NP9 (Aubry *et al.*, 1996).

The base of C24n.3n has been putatively identified in two separate paleomagnetic studies in different parts of the Bighorn Basin. Tauxe *et al.* (1994), working in the Antelope Creek/Elk Creek section of the central Bighorn Basin, correlated a normal polarity zone (their N2) beginning at 312 m above the inferred Wa0 red beds with the base of C24n.3n. Clyde *et al.* (1994), working in the Foster Gulch/McCullough Peaks section in the northern Bighorn Basin, found a normal polarity zone (their C+) beginning 950 m above the Wa0 red beds. They interpreted this zone as equivalent to the beginning of C24n.3n. In both the Clyde *et al.* (1994) and Tauxe *et al.* (1994) studies, mammalian fossils were recovered from the rocks recording the polarity transition. In the Antelope Creek/Elk Creek section, these faunas lack the index fossil *Bunophorus*, which first occurs at 365 m, 53 m higher than the polarity transition (Bown *et al.*, 1994a). In the Foster Gulch/McCullough Peaks section, the first occurrence of *Bunophorus* is 50 m below the polarity transition. Thus the *Bunophorus* FAD and the magnetic polarity data are not consistent between the two sections. The Polecat Bench/Clarks Fork Basin section records the same relationship between the FAD *Bunophorus* and magnetic polarity events that is seen in the Foster Gulch/McCullough Peaks section, that is, there is no normal polarity interval below the FAD of *Bunophorus* but above the base of the Wasatchian (Butler *et al.*, 1981), although paleomagnetic sampling density is low in this part of the section.

Biostratigraphic relationships also are not consistent between the northern and central Bighorn Basin. The last occurrences of *Haplomylus* and *Ectocion* are above the first occurrence of *Bunophorus* in the Antelope Creek/Elk Creek section, whereas in both the Clarks Fork Basin and Foster Gulch/McCullough Peaks sections their ranges do not overlap *Bunophorus* (Bown *et al.*, 1994a; Clyde, 1997). This is probably the result of stratigraphic condensation in the Antelope Creek/Elk Creek section that results from local cut-and-fill deposits (Bown *et al.*, 1994a), although it could also result from lower sample density in the northern sections, or real differences in temporal range.

Because the Foster Gulch/McCullough Peaks section is much thicker than the Antelope Creek/Elk Creek section, displays more stable magnetic behavior (Clyde *et al.*, 1994), and agrees with the Polecat Bench/Clarks Fork Basin section, we think it is more likely that the reversal reported by Tauxe *et al.* (1994) at the 312 m level of the Antelope Creek/Elk Creek section is a spurious normal overprint

than that Clyde *et al.* (1994) missed a normal event. Indeed Tauxe *et al.* (1994, p. 165) raised the possibility that some or all of the normal polarity intervals in the Antelope Creek/Elk Creek section are overprints. Consequently we have chosen to disregard the paleomagnetism of Tauxe *et al.* (1994) for the middle part of the section.

The youngest of the tie points in the Bighorn Basin is a radiometric age of 52.8 ± 0.3 Ma derived from a bentonitic tuff at the 634 m level of the Antelope Creek/Elk Creek section (Wing *et al.*, 1991). The date is based on $^{40}\text{Ar}/^{39}\text{Ar}$ analysis of sanidine. The ash is 53 m above the first occurrence of *Lambdaotherium*, which indicates the base of the Lostcabinian land mammal assemblage zone (Bown *et al.*, 1994a). The FAD of *Lambdaotherium* is also recorded at the 1420 m level of the Foster Gulch/McCullough Peaks section, where it occurs 20 m above the top of a normal polarity interval inferred to be 24n.2n (Clyde *et al.*, 1994). Given Cande and Kent's (1995) estimate of 52.76 Ma for the top of 24n.2n, the FAD of *Lambdaotherium* is approximately synchronous in the northern and central Bighorn Basin.

Although the discussion above reveals several sources of uncertainty in our calibration points to a global geochronology, we note that the order of magnetic, geochemical, and biological events is robust. Varying interpretations of the magnetic stratigraphy affect the inferred ages of climatic and biotic changes by only a few hundred thousand years or less, which is unlikely to affect interpretation of climatic and biotic changes. For example, we have interpolated numerical ages for four biostratigraphic events (Biohorizon A, Biohorizon B, *Heptodon* FAD, *Lambdaotherium* FAD) in two separate composite sections (Tables 7.2–7.4). For no event do the interpolated ages deviate from one another by more than 174 ka between the different sections (Biohorizon A – 73 ka, Biohorizon B – 120 ka, *Heptodon* FAD – 125 ka, *Lambdaotherium* FAD – 174 ka), in spite of the potential for the age estimates to be affected by sampling intensity as well as by incorrect calibration of the sections.

Age calibration of the Polecat Bench/Clarks Fork Basin, Foster Gulch/McCullough Peaks, and Antelope Creek/Elk Creek sections reveals variation in rock accumulation rates within and among sections (Fig. 7.2, Tables 7.2–7.4). The more northerly sections have higher rates, probably because they are also further west and closer to the structural axis of the basin. Both the Antelope Creek/Elk Creek and Foster Gulch/McCullough Peaks sections show increasing rates of accumulation up section. The lower parts of both composite sections are closer to the margin of the basin, and their upper parts are closer to the center, so increases in accumulation rate within long composite sections may reflect position in the basin more than climatic or tectonic change through time (Clyde, 1997). Based on the relative thickness of mammalian biostratigraphic zones, Gingerich (1983) argued that maximum rates of basin subsidence occurred during the late Clarkforkian.

The Antelope Creek/Elk Creek section shows nearly a twofold increase in rock accumulation rate from the lower 365 m to the upper 270 m, which seems high in light of the continuity of mudstone and sandstone deposition throughout. However, there is independent evidence for increased sediment accumulation rates in the middle of the section. Bown and Kraus (1993) and Kraus and Bown (1993)

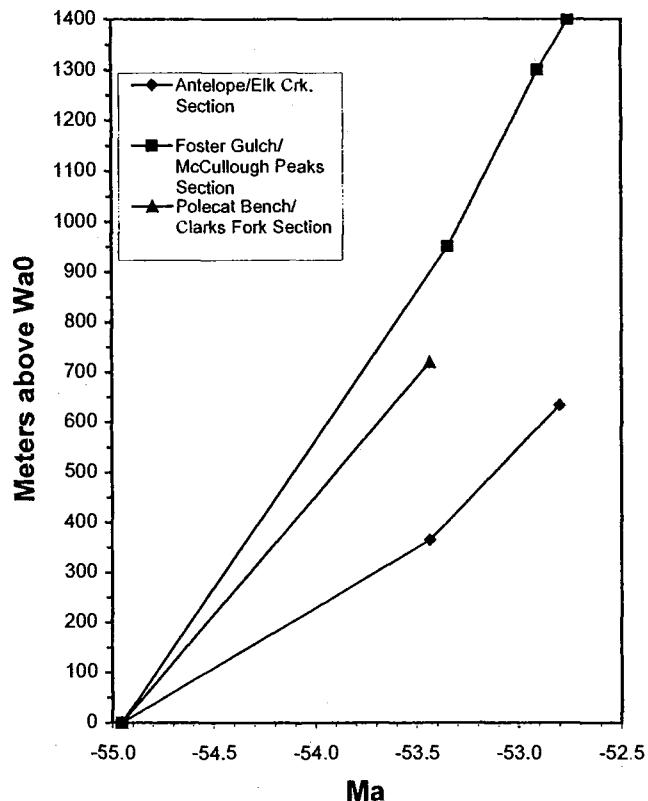


Figure 7.2. Rock accumulation rates in the three major stratigraphic sections across the Paleocene–Eocene transition in the Bighorn Basin. Rates calculated using age model 1 (see text). Calibrations for sections in Tables 7.2–7.4.

pointed out that there was a substantial decrease in paleosol maturity in the middle of the Antelope Creek/Elk Creek section, implying an increase in frequency and size of overbank depositional events. Our confidence in the age calibration of the Antelope Creek/Elk Creek section is also reinforced by the observation of similar-sized shifts in accumulation rates in the other composite sections (Fig. 7.2, Tables 7.2 and 7.4). Finally, our decision to disregard the paleomagnetism of Tauxe *et al.* (1994) for the middle part of the Antelope Creek/Elk Creek section decreases the difference in accumulation rates between the lower and upper half of the section. If we follow Tauxe *et al.* (1994) in placing the top of C24r at 312 m, this implies a threefold increase in accumulation rate within the Antelope Creek/Elk Creek section. In summary, rates of rock accumulation and comparisons between Bighorn Basin sections suggest that our age calibrations are robust and unlikely to change substantially unless ages for the paleomagnetic timescale or the carbon isotope excursion are modified.

PALEOCLIMATIC AND PALEOHYDROLOGIC RECONSTRUCTION

Leaf margin analysis

Leaf margin analysis is based on the observation made on living vegetation that the proportion of dicotyledonous species with entire-margined (untoothed) leaves is directly correlated with mean annual temperature (Wolfe, 1979). The functional basis of this correlation is not fully understood, but the primitive condition in dicots is probably to have entire-margined leaves, and teeth have evolved independently in many lineages (Hickey and Wolfe, 1975). Experimental studies suggest that teeth on leaves serve a variety of functions. In some temperate deciduous species teeth are photosynthetically active soon after bud-break, and long before the main part of the lamina (Brosh-Baker and Peet, 1997). Early photosynthetic activity in teeth may allow leaves to export photosynthate to the rest of the plant earlier in the year, a potential advantage in climates with short growing seasons and therefore a brief period during which the leaf can be a net source of energy (Baker-Brosh and Peet, 1997). Teeth have also been observed to be points of rapid transpirational water loss even after the leaf is fully expanded, presumably because tooth apices are associated with vascular tissue and emerge through the boundary layer of humid air that surrounds the lamina (Canny, 1990). Rapid loss of water through tooth apices suggests that teeth have a cost in terms of water loss as well as a benefit in terms of more rapid expansion and photosynthetic activity at the beginning of the growing season. The prevalence of teeth in a local flora probably represents a balance between the transpirational cost and the photosynthetic benefit that depends on a combination of local temperature, precipitation, and humidity. This hypothesis is consistent with the rarity of toothed leaves in wet and dry tropical and subtropical forests, where accelerated water loss under high temperatures could lead rapidly to wilting, and also with the rarity of teeth in cold, low-productivity environments where low nutrient levels have a similar effect to water stress (Givnish, 1979).

As with any correlational method, the use of leaf margin proportion (P) to infer mean annual temperature (MAT) makes the uniformitarian assumption that there was the same relationship between P and MAT in the past as has been observed in the present. In other words we assume that the leaves of plants in the early Cenozoic evolved morphological responses to climate in the same way that they do today. We think this assumption is valid for three reasons. Firstly, the evolution of teeth appears to hinge on basic ecophysiological relationships that affect all dicots: optimizing the rate of photosynthesis under a given temperature and precipitation regime. Thus the same factors that influence leaf morphology today operated in similar ways in the past. Secondly, the evolutionary change from entire to toothed leaves (and back) appears to be a relatively easy transition – both toothed and entire species are found within many living genera, and the variety of anatomical patterns in teeth implies that they have evolved many times within the dicotyledons (Hickey and Wolfe, 1975). The evolutionary lability of teeth makes it unlikely that the relationship between teeth and climate in the early Cenozoic would have been very different owing to a different set of lineages being present. There appears to be a high capacity for leaf form to respond to climate through evolution. Thirdly, the

early Cenozoic floras analyzed here contain a substantial proportion of extant genera and families, many of which are in the East Asian and North American data sets used to calibrate the MAT/ P relationship. Even if there were phylogenetic constraints on the development of teeth (e.g., if some dicot lineages do not evolve teeth no matter what climatic conditions they live under), these constraints should be similar for early Cenozoic and extant floras of the northern hemisphere because the floras of the two times are taxonomically similar.

The correlation between MAT and P has been quantified for a group of 34 sites in East Asia (Wolfe, 1979), for two separate groups of sites from the Americas (Wolfe, 1993; Wilf, 1997), and for one set of sites from Australia (Greenwood, 1992). The three northern hemisphere data sets demonstrate similar relationships between P and MAT (Wilf, 1997). The 34 sites in the East Asian data set show the strongest correlation of P with MAT ($r = 0.98$, $p < 0.001$), perhaps because they were drawn from areas with adequate growing season precipitation (Wolfe, 1979), and because of the large number of species per sample (Wilf, 1997). The correlation of P with MAT in the largely North American Climate–Leaf Analysis Multivariate Program (CLAMP) data set (106 sites; Wolfe, 1993) is less precise, although still highly significant ($r^2 = 0.76$, $p < 0.0005$). The lower correlation of P with MAT in the CLAMP data set may reflect the large number of samples from dry and extremely cold sites, and also the smaller number of species per site (Wilf, 1997). The leaf margin data set assembled by Wilf (1997) includes nine sites from North and South America and the Caribbean, and demonstrates a correlation between P and MAT that has a slope and intercept very similar to that seen in the East Asian data sets ($r^2 = 0.94$, $p < 0.0005$). The slope and intercept for the Australian data set are different from any of the northern hemisphere data (MAT = $6.4176 + [17.63P]$), and the r^2 value is 0.78 (Greenwood, 1992; Greenwood, personal communication, 1997). The different relationship between P and MAT in Australian vegetation may reflect factors such as greater seasonality of rainfall and lower soil nutrient levels in Australian forests, or strong phylogenetic control of leaf morphology in some southern hemisphere lineages.

The estimates of MAT in this paper are based on the East Asian data set of Wolfe (1979) using the regression equation

$$\text{MAT} = 1.14 + (30.6P), \quad (7.1)$$

where P is the proportion of entire-margined species in the assemblage. We use the East Asian data set to make our temperature estimates because it is climatically the most analogous to the early Cenozoic of the Bighorn Basin in lacking extremely cold or dry sites. The standard error of the estimate of MAT based on Wolfe's (1979) data is 0.8°C (Wing and Greenwood, 1993), but this is not the only component of error. Wilf (1997) has pointed out that there is also binomial error caused by uncertainty in estimating the true proportion of entire-margined species for the whole regional flora based on a sample with a finite number of species. This error (σ) is calculated in $^\circ\text{C}$ by

$$\sigma = 30.6\sqrt{P(1-P)/r}, \quad (7.2)$$

where P is the proportion of entire-margined species in the sample, r is the total number of species in the sample, and the constant 30.6 is the regression coefficient for the East Asian data set (Wilf, 1997). For samples with 25–60 species and equal proportions of entire and non-entire forms, binomial sampling error creates a 2–3 °C uncertainty in estimating MAT (Wilf, 1997).

The accuracy of leaf margin analysis may also be affected by taphonomic processes that bias the representation of entire vs. toothed leaves, although no such effect has been demonstrated in actualistic studies (e.g., Greenwood, 1982). In addition, MacGinitie (1969) reported that toothed species are more common in stream-side vegetation than the regional vegetation in extant subtropical forests. This observation has not been quantified, but to the extent that it is true, fluvially deposited leaf assemblages may tend to underestimate MAT systematically.

Oxygen isotope geochemistry

In temperate and polar regions the mean oxygen isotope composition ($\delta^{18}\text{O}$ value*) of meteoric water (e.g., precipitation such as rain and snow) is strongly correlated with MAT, with the ^{18}O -depleted values in cold regions and ^{18}O -enriched values in warm regions (Dansgaard, 1964). The relationship between temperature and meteoric water $\delta^{18}\text{O}$ value results from the formation of vapor masses in warm, low-latitude regions, followed by rainout from these masses in colder, high-latitude regions, a phenomenon which has been successfully modeled as a Rayleigh distillation process (Dansgaard, 1964; Rozanski *et al.*, 1993). In tropical areas, meteoric water $\delta^{18}\text{O}$ values are more strongly correlated to the amount of precipitation than to MAT. Complexities due to differences in vapor sources, orographic effects, and monsoonal climates can affect these relationships. However, the positive correlation between temperature and the $\delta^{18}\text{O}$ of meteoric water should have been present in temperate and polar regions in the geologic past. Changes in meteoric water $\delta^{18}\text{O}$ value provide a monitor of major, regional changes in the climatic and hydrologic cycle.

Our monitor of meteoric water $\delta^{18}\text{O}$ value is the isotopic composition of authigenic minerals in paleosols. The $\delta^{18}\text{O}$ of a mineral is determined by the fractionation of oxygen isotopes between the solid phase and the water from which it forms (which commonly varies as a function of temperature) and the $\delta^{18}\text{O}$ of the water. Thus minerals that form in near-surface environments record the isotopic composition of surface water, which will track the $\delta^{18}\text{O}$ of meteoric water to a greater or less extent. Pedogenic and vein-filling calcites have been used extensively as proxies for surface water $\delta^{18}\text{O}$ values (e.g., Quade *et al.*, 1989; Winograd *et al.*, 1992; Cerling and Quade, 1993). The oxygen isotope compositions of clay minerals and oxides in soils have been used increasingly to monitor the $\delta^{18}\text{O}$ of surface water (Savin and Epstein, 1970; Lawrence and Taylor, 1972; Yapp, 1987, 1993; Bird *et al.*, 1992, 1993).

* $\delta^{18}\text{O} = ((R_{\text{sample}}/R_{\text{standard}}) - 1) \times 1000$, where R is the $^{18}\text{O}/^{16}\text{O}$ in the sample or standard. The standard is Vienna standard mean ocean water (V-SMOW). The units are in per mil (‰).

Vertebrate fossils encrusted with hematite ($\alpha\text{-Fe}_2\text{O}_3$) are common in alluvial paleosols that developed on fluvial sediments that accumulated in the Bighorn Basin during the late Paleocene and early Eocene (Bown and Kraus, 1981*a,b*). Based on the number of paleosols, the timespan of sediment accumulation, and paleosol maturity, it has been estimated that individual paleosols formed in thousands to tens of thousand of years (Bown and Kraus, 1993; Kraus and Bown, 1993). A thorough examination of the timing of hematite mineralization within paleosols is beyond the scope of this paper (see Bao *et al.*, 1998), but several lines of evidence provide some constraint. High concentrations of hematite are found only as encrustations on vertebrate fossils, not in the soil matrix or on nodules. Not all fossils have hematite coatings; encrustation is closely associated with fossils from hydromorphic paleosols, particularly 'class A' gray mudstones (Bown and Kraus, 1981*b*; Bown *et al.*, 1994*a*). Petrographic observations of overgrowth relationships demonstrate that iron oxide and micrite were deposited synchronously, and that both were deposited prior to void-filling sparry calcite. Oxygen isotope analysis indicates that micrites are near-surface, pedogenic products, whereas sparry calcites are deep-burial products (Koch *et al.*, 1995). These observations suggest that initial iron oxide formation occurred in near-surface environments. The initial precipitate was probably ferrihydrite ($5\text{Fe}_2\text{O}_3 \cdot 9\text{H}_2\text{O}$), a highly disordered and poorly crystalline precursor, that was subsequently altered by dehydration and internal rearrangement to hematite (Johnston and Lewis, 1983; Schwertmann and Murad, 1983; Schwertmann and Taylor, 1989), or insoluble Fe-organic complexes, which were transformed into hematite by oxidation (McKeague *et al.*, 1986).

Several characteristics of iron oxides make them ideal for reconstruction of the $\delta^{18}\text{O}$ of the surface water. Iron oxides hold their original oxygen isotope compositions with high fidelity; even drastic chemical treatments do not affect the $\delta^{18}\text{O}$ of hematite and goethite (Becker and Clayton, 1976; Yapp, 1991). In addition, there is evidence that oxygen isotope fractionation between water and hematite is relatively insensitive to temperature change in the surface temperature range (Clayton and Epstein, 1961; Zheng, 1991), though the fractionation relationship determined by Yapp (1990*a*) shows greater temperature sensitivity. The source of this discrepancy is under investigation, but in any case the fractionation of oxygen isotopes between water and hematite is much less sensitive to temperature than the water/calcite fractionation. Consequently, hematite is an excellent indicator of the $\delta^{18}\text{O}$ of ancient surface water. Finally, recent papers by Yapp (1987, 1990*a,b*, 1991, 1993, 1997) have demonstrated the utility of oxygen isotope analysis of iron oxides and addressed many questions associated with their genesis and analysis.

MATERIALS AND METHODS

Leaf margin analysis

Fossil assemblages for leaf margin analysis come from >250 sites in the Fort Union Formation and Willwood Formation of the Bighorn Basin that have been collected by field parties from the Smithsonian Institution and Yale University. Most assemblages come from small quarries of $\sim 3 \times 3$ m laterally and less than 0.5 m

stratigraphic thickness. These sites occur in all parts of the Bighorn Basin, but are concentrated in the areas around North Butte, Elk Creek, and upper Fifteenmile Creek, and in the Clarks Fork Basin (Fig. 7.1; Hickey, 1980, Brown *et al.*, 1994a; Wing *et al.* 1995, Wing, 1998). Most of the localities are in measured sections that can be correlated lithostratigraphically to the carbon isotope excursion and LPTM.

Most of the leaf assemblages examined for this study were collected from carbonaceous shales that accumulated as the result of fine-grained sedimentation events on poorly drained distal floodplains (Davies-Vollum and Wing, 1998). Backswamp leaf assemblages are largely autochthonous, representing only a very small area of floodplain vegetation (Davies-Vollum and Wing, 1998). Grain size, bed forms, and thin-section features are consistent with low-energy deposition, and typically riparian genera such as *Platanus* are rare in the backswamp assemblages (Wing *et al.*, 1995). The fossil plant assemblage from any given backswamp site probably accumulated during one or a few sedimentation events spread over no more than a few years, and carbonaceous beds of 1–3 m thickness probably accumulated over hundreds to thousands of years (Davies-Vollum and Wing, 1998). Thus time averaging within or among sites along a single bed is insignificant for the purposes of this study.

A smaller number of floral assemblages come from abandoned channel and near-channel settings. Current energy in the near-channel environments was greater than in the backswamps or abandoned channels, but identifiable leaves still appear to be derived from local vegetation (Wing *et al.*, 1995). Temporal and spatial averaging of individual near-channel and abandoned channel floras is probably on the order of years and hundreds of meters. Many of these assemblages are dominated in numbers of specimens by typical riparian genera such as *Platanus*, but they contain a diversity of other, non-riparian species as well.

In order to increase the number of species for each leaf margin estimate of MAT, and hence decrease the effect of sampling error on the temperature estimate (Eq. 7.2), we have lumped floras from stratigraphic intervals of varying thickness for each estimate. This process introduces analytical time averaging on the order of hundreds of thousands of years, which means that temperature fluctuations of less than that duration cannot be discerned.

There are a total of eight leaf margin estimates of MAT derived from Bighorn Basin floras, designated Leaf Margin Analysis (LMA)-1 through LMA-8 (Table 7.6). All 14 of the early Clarkforkian sites that were included in LMA-1 were collected from the Fort Union Formation in the Clarks Fork Basin in northernmost Wyoming or southernmost Montana (Hickey, 1980). Some of these sites can be correlated with meter levels in the Polecat Bench/Clarks Fork Basin composite section, while the remainder can be assigned to the Cf1 faunal zone based on nearby mammalian faunal collections (Hickey, 1980). The most extensive collection from the early Clarkforkian is from the Bear Creek Mine and Foster Gulch (Montana) area. Although this locality is not in the Polecat Bench/Clarks Fork Basin composite section, it can be dated biostratigraphically because of the occurrence of early Clarkforkian mammals in the roof shales that are stratigraphically close to the flora (Hickey, 1980). The Bear Creek fauna may be somewhat earlier in the

Table 7.6. Leaf margin estimates of MAT

Sample	Sections with samples*	Meter level	Age model 1	Age model 2	Duration	MAT	MAT error	No. of entire spp.	No. of toothed spp.
LMA-8	ECS	621	-52.831	-52.842	0.01	22.2	2.0	33	15
LMA-7 (midpoint)	ECS	444	-53.249	-53.411	0.11	15.8	2.2	23	25
LMA-6 (midpoint)	ECS	332	-53.573	-53.806	0.17	10.8	3.3	6	13
LMA-5 (midpoint)	ECS	155	-54.310	-54.568	0.37	16.4	2.7	16	16
LMA-4 (midpoint)	ECS	57.5	-54.715	-54.987	0.40	18.2	2.3	24	19
LMA-3 (midpoint)	HCS, ECS, MPS	-37	-55.109	-55.393	0.25	15.7	2.4	20	22
LMA-2 (midpoint)	CFB, WES	-123	-55.467	-55.763	0.33	15.8	2.2	24	26
LMA-1 (midpoint)	CFB, Bear Creek	1000	-56.040	-56.347	0.62	12.9	2.4	15	24

*Section abbreviations as in Table 7.1; models 1 and 2 are explained in the text.

Clarkforkian than the Cf1 faunas collected near Polecat Bench (J. Alroy, personal communication, 1997), and therefore LMA-1 may include floras that span the entire early Clarkforkian, an interval we infer to be as much as 610 ka (Tables 7.4 and 7.5).

Floras collected at 30 sites were combined for LMA-2. Four of the sites are located in the Clarks Fork Basin, where they are associated with mammals of zone Cf2 and can be correlated to the Polecat Bench/Clarks Fork Basin section. The other 26 sites are in the Fort Union Formation in the North Butte, Worland East, Sand Creek Divide, and Antelope Creek areas of the eastern and southern Bighorn Basin. These sections lack age-diagnostic mammalian fossils or magnetostratigraphy, so floral sites were assigned to LMA-2 based on their stratigraphic level with respect to the Wa0 red bed. Sites that were 75–165 m below the Wa0 red bed were assigned to LMA-2. If we assume that accumulation rates in the upper Fort Union Formation of the eastern Bighorn Basin were the same as those in the lower Willwood Formation in the same area (0.23 m ka^{-1} ; Table 7.2), then these meter levels correspond to the upper and lower bounds of Cf2 time as determined from the age calibration of the Polecat Bench/Clarks Fork Basin section (Table 7.4). Although we lack dated horizons in the Fort Union of the eastern Bighorn Basin, the assumption of constant rates of rock accumulation during the middle Clarkforkian through early Wasatchian in this area is consistent with other evidence. Firstly, the areas from which the floras were collected are all distributed along strike near the margin of the basin, which should favor similar low rates of rock accumulation in all sections. Secondly, the Fort Union Formation in the eastern Bighorn Basin rests on a major erosional unconformity developed on the Late Cretaceous Lance Formation and Meeteetse Formation, but is gradational with the overlying Willwood Formation. This is consistent with Fort Union Formation deposition beginning in the late Paleocene and continuing without substantial hiatus into the early Eocene. Thirdly, the composition of the megaflores indicates a late Paleocene age (Wing, 1998). Fourthly, scattered mammalian fossils from near the base of the Fort Union Formation west of Greybull are Tiffanian or Clarkforkian (Gingerich, personal communication, 1990). Clearly, more paleomagnetic, radiometric, or biostratigraphic data are needed in the Fort Union Formation sections of the eastern Bighorn Basin, but in the absence of such data we think the stratigraphic grouping used here is likely to be a close approximation of Cf2 time. Sites grouped for LMA-2 span 480 ka (Tables 7.4 and 7.6).

Floras from 35 sites were combined for LMA-3. One of these sites is in the Clarks Fork Basin and can be correlated directly with the Polecat Bench/Clarks Fork Basin section and Cf3 mammals (Hickey, 1980). The remaining 34 sites are from the uppermost 75 m of the Fort Union Formation in the North Butte, Worland East, Gould Butte, and Antelope Creek areas. As with the sites used for LMA-2, rock accumulation rates for the lower part of the Antelope Creek/Elk Creek section were assumed to apply to the uppermost Fort Union Formation. Fifteen of the sites are 30 m or less below the Wa0 red bed in conformable sequence. The lower bound for LMA-3 sites was set at 75 m below the Wa0 red bed because this is the level that is age equivalent to the base of Cf3 (Tables 7.3 and 7.4) if a depositional rate of 0.23 m ka^{-1} is assumed. Sites grouped for LMA-3 span 300 ka.

LMA-4 is based on floras from 20 sites in the Antelope Creek, Gould Butte, and Foster Gulch areas. The sites in the Antelope Creek/Elk Creek section are all 10–100 m above the Wa0 red bed, the site from Foster Gulch is 18 m above the Wa0 red bed, and the sites from the Gould Butte area are from a stratigraphic interval 20–105 m above the first appearance of Eocene plant megafossils. Based on rock accumulation rates calculated from the lower part of the Antelope Creek/Elk Creek section (Table 7.3), sites grouped for LMA-4 span 410 ka.

The remaining leaf margin analyses (LMA-5 through LMA-8) are based almost exclusively on floras from the Antelope Creek/Elk Creek section. Most of the 31 sites from which floras were combined for analysis in LMA-5 have stratigraphic levels of 110–200 m in the Antelope Creek/Elk Creek section, except for one diverse site in the Gould Butte area that is about 200 m above the first occurrence of Eocene plants. Based on rock accumulation rates calculated from the lower part of the Antelope Creek/Elk Creek section (Table 7.3), sites grouped for LMA-5 span 390 ka.

The LMA-6 is based on floras from only six sites, all between 311 and 353 m in the Antelope Creek/Elk Creek section. Based on rock accumulation rates calculated from the lower part of the Antelope Creek/Elk Creek section (Table 7.3), sites grouped for LMA-6 span 180 ka.

The LMA-7 is also based on floras from six sites in a narrow stratigraphic interval, 420–468 m above the Wa0 red bed. Rock accumulation rates calculated for the upper part of the Antelope Creek/Elk Creek section (Table 7.3) indicate that the sites grouped for LMA-7 span 100 ka. The stratigraphically highest temperature estimate, LMA-8, is derived from the flora of a single, laterally extensive carbonaceous shale at the 621 m level of the Antelope Creek/Elk Creek section. This is only 13 m below the bentonitic tuff (52.8 ± 0.3 Ma). There are 24 sites in this bed distributed across about 10 km of outcrop. The estimated maximum timespan for LMA-8, 10 ka, is based on depositional models discussed by Davies-Vollum and Wing (1998).

Oxygen isotope analysis

We obtained samples spanning the Clarkforkian to middle Wasatchian from fossil mammals collected in the southern and central Bighorn Basin (United States Geological Survey, Denver) and the Clarks Fork Basin (Museum of Paleontology, University of Michigan). Details of the isotopic analysis of hematite are fully explained in Bao *et al.* (1998). Briefly, hematite was collected from bones by drilling under a microscope. Samples were pretreated with 1 M HCl (24–36 h) and dilute NaHCl (12–24 h) at room temperature to remove calcite, apatite, clay minerals, and organic contaminants. To obtain $\delta^{18}\text{O}$ values for hematite, which is intimately mixed with silicate minerals, we used a modified version of the mass-balance approach of Bird *et al.* (1992). Firstly, samples were treated with 5 M NaOH at 95 °C (3–10 h). This treatment removes a large fraction of the silicates and concentrates hematite, but has no effect on the $\delta^{18}\text{O}$ of hematite (Yapp, 1991). The pretreated bulk sample was split, and one split was treated with 6 M HCl at 80 °C (<30 min), leaving a

residue of silicate minerals, chiefly quartz. The $\delta^{18}\text{O}$ of pure hematite was calculated using the following relationship:

$$\delta^{18}\text{O}_{\text{bulk}} = \delta^{18}\text{O}_{\text{hematite}} * f_{\text{Fe}} + \delta^{18}\text{O}_{\text{residue}} * (1 - f_{\text{Fe}}), \quad (7.3)$$

where $\delta^{18}\text{O}_{\text{bulk}}$ is the measured isotope composition of pretreated bulk powder, $\delta^{18}\text{O}_{\text{residue}}$ is the composition of the silicate residue, and f_{Fe} and $1 - f_{\text{Fe}}$ are the oxygen mole fractions of hematite and silicates, respectively, in pretreated bulk powder.

To calculate mole fractions, the concentrations of Fe, Si, and Al (the concentrations of other elements are trivial) were determined for the split of the pretreated bulk powder by inductively coupled plasma atomic emission spectroscopy (ICP-AES) using a Perkin Elmer 6000. The error associated with elemental analysis for each sample was determined by analyses of duplicates. The mean value for error was ± 0.0007 ($n = 29$) for the oxygen mole fraction in hematite (≈ 1 weight %). This analysis was conducted at the Department of Geosciences, Princeton University.

The $\delta^{18}\text{O}$ value of pretreated bulk powder and silicate residues was determined by laser fluorination. Approximately 1–2 mg of sample powder was loaded into a stainless steel holder, then pretreated overnight with BrF_5 at room temperature to remove adsorbed atmospheric moisture and gases. Oxygen was generated by fluorination with a 20 W CO_2 laser in a BrF_5 atmosphere (Valley *et al.*, 1995; Rumble *et al.*, 1994). The O_2 evolved by laser fluorination was collected on a molecular sieve at -190°C , then immediately analyzed as O_2 on a Finnigan MAT 252. The error associated with laser fluorination and isotopic analysis was assessed through analysis of duplicates. The mean value for error was $< 0.15\%$. Laser fluorination and oxygen isotope analysis on a Finnigan MAT 252 were conducted at the Geophysical Laboratory, Carnegie Institution of Washington.

The error for each calculated value of $\delta^{18}\text{O}_{\text{hematite}}$ was estimated from the error in determination of weight % hematite. The mean value for the effect of this error on $\delta^{18}\text{O}_{\text{hematite}}$ was $\pm 0.26\%$ ($n = 29$). The average for the total analytical error, which also includes errors associated with isotopic analysis, was $\pm 0.7\%$.

To test the reliability of the method, whole process replicate analyses (performed on separate sample powders drilled from the same bone) were conducted on two samples: HOA-YPM350 and HOA-SC90. The differences in $\delta^{18}\text{O}_{\text{hematite}}$ were 0.11‰ and 0.45‰ for these whole process duplicates. Data consistency was tested through comparisons of values between localities at different lateral positions at the same meter level: SC4 and SC123 at 1570 m in the Polecat Bench/Clarks Fork Basin section, and D1300 and D1301 at 78 m in the Antelope Creek/Elk Creek section. Differences in $\delta^{18}\text{O}_{\text{hematite}}$ for different samples from the same meter level were 0.84‰ and 1.2‰.

PALEOCLIMATIC RESULTS

Mean annual temperature from leaf assemblages

The eight estimates of MAT (LMA-1 through LMA-8) are shown in Table 7.6 and plotted against time in Fig. 7.3. Durations associated with each estimate are

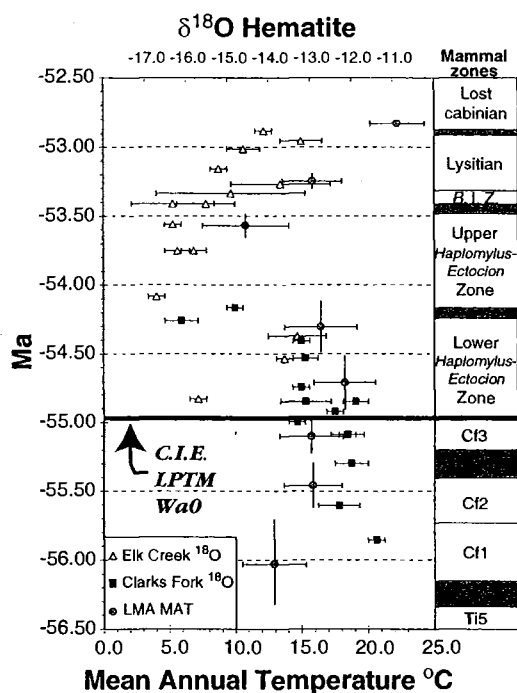


Figure 7.3. Temperature estimates from leaf margin analysis (LMA) and estimates of the $\delta^{18}\text{O}$ of precipitation from iron oxides plotted against time. C.I.E., carbon isotope excursion; LPTM, Latest Paleocene Thermal Maximum; B.I.Z., *Bunophorus* Interval Zone.

discussed above. MAT estimates were calculated using Equation (7.1) and errors of the MAT estimates were calculated using Equation (7.2).

MAT estimates rise from 12.9 to 15.3 °C during the Clarkforkian. The earliest Wasatchian estimate of MAT is 18.2 °C, after which MAT declines to 16.4 °C and then 10.8 °C at an interpolated age of 53.56 Ma (uppermost C24r). The coldest MAT estimate has a relatively large uncertainty (± 3.3 °C) because of the low diversity of the flora from this time period. This cold estimate of MAT is as low as the mid-Paleocene (Tiffanian) MAT estimates made by Hickey (1980). In the middle Wasatchian, MAT estimates rise first to 15.8 °C and finally to 22.2 °C by 52.83 Ma, near the beginning of the Lostcabinian and C24n.1n.

Although the small number of MAT estimates and the large amount of analytical time averaging for the Clarkforkian estimates do not make for a detailed record of temperature change through time, a strong pattern emerges from the data. MAT rose during the last million years of the Paleocene and into the early Eocene, declined to less than late Paleocene values by about 1.5 Ma following the carbon isotope excursion, and then warmed rapidly over the succeeding 700 ka to reach a long-term maximum in the middle to later early Eocene.

Table 7.7. $\delta^{18}\text{O}$ of hematite-encrusting bones

Sample	Section*	Meter level	Age model 1	Age model 2	$\delta^{18}\text{O}$ hematite	Error
HOA-YPM33	ECS	601	-52.878	-52.906	-14.1	0.2
HOA-YPM1	ECS	571	-52.949	-53.002	-13.2	0.5
HOA-D1467	ECS	546	-53.008	-53.083	-14.6	0.4
HOA-D1531	ECS	485	-53.152	-53.279	-15.2	0.2
HOA-D1398	ECS	438	-53.263	-53.430	-13.7	1.2
HOA-D1454	ECS	409	-53.332	-53.523	-14.9	1.8
HOA-D1300	ECS	378	-53.405	-53.623	-16.3	1.0
HOA-D1301	ECS	378	-53.405	-53.623	-15.5	0.7
HOA-D1374	ECS	336	-53.556	-53.789	-16.3	0.2
HOA-YPM350R	ECS	290	-53.748	-53.987	-16.2	0.3
HOA-YPM350	ECS	290	-53.748	-53.987	-15.8	0.3
HOA-YPM290	ECS	210	-54.081	-54.331	-16.7	0.2
HOA-YPM104	ECS	140	-54.372	-54.632	-13.3	0.7
HOA-YPM119	ECS	100	-54.539	-54.804	-13.6	0.2
HOA-YPM115	ECS	30	-54.830	-55.105	-15.7	0.2
HOA-SC232	CFB	1895	-54.164	-54.417	-14.8	0.2
HOA-SC34	CFB	1850	-54.259	-54.515	-16.1	0.4
HOA-SC313	CFB	1780	-54.406	-54.667	-13.2	0.2
HOA-SC12	CFB	1720	-54.533	-54.798	-13.1	0.3
HOA-SC18	CFB	1620	-54.744	-55.016	-13.2	0.2
HOA-SC4	CFB	1570	-54.849	-55.125	-11.9	0.3
HOA-SC123	CFB	1570	-54.849	-55.125	-13.1	0.6
HOA-SC40	CFB	1535	-54.923	-55.201	-12.4	0.2
HOA-SC138	CFB	1500	-54.997	-55.278	-13.3	0.2
HOA-SC90	CFB	1455	-55.092	-55.376	-12.1	0.2
HOA-SC90R	CFB	1455	-55.092	-55.376	-12.1	0.4
HOA-SC127	CFB	1355	-55.303	-55.594	-12.0	0.4
HOA-SC92	CFB	1210	-55.609	-55.910	-12.3	0.5
HOA-SC171	CFB	1090	-55.862	-56.171	-11.4	0.2

*Section abbreviations as in Table 7.1; models 1 and 2 are explained in the text.

Isotopic composition of hematite

Hematite $\delta^{18}\text{O}$ values are given in Table 7.7 for samples from the Clarks Fork Basin and the eastern and central Bighorn Basin. In Fig. 7.3, hematite $\delta^{18}\text{O}$ values are plotted vs. age for comparison with the MAT estimates derived from leaf margin analysis. In the Clarks Fork Basin, hematite $\delta^{18}\text{O}$ values are fairly consistent from 55.86 Ma (1090 m) to 54.43 Ma (1780 m), then drop $\sim 3\text{‰}$ by 54.27 Ma. In the central Bighorn Basin, the $\delta^{18}\text{O}_{\text{hematite}}$ at 54.39 Ma (140 m) is nearly identical to that observed at 54.43 Ma in the Clarks Fork Basin. As in the north, $\delta^{18}\text{O}_{\text{hematite}}$ dropped by $\sim 3.5\text{‰}$ by 54.09 Ma (210 m) in the Antelope Creek/Elk Creek section. Values remained low for over 500 ka before beginning to rise between 53.36 Ma (378 m) and 53.11 Ma (409 m).

Given independent evidence that hematite forms in the pedogenic environment (Bao *et al.*, 1998), $\delta^{18}\text{O}_{\text{hematite}}$ can be used to infer relative changes in the $\delta^{18}\text{O}$

of surface water in the Bighorn Basin. Current uncertainty regarding the correct fractionation relationship for the hematite/water system precludes reconstruction of the absolute $\delta^{18}\text{O}$ value of surface water. However, all three published fractionation relationships exhibit low temperature sensitivity in the earth surface temperature range. Estimates of sensitivity range from $0.14\text{‰}\text{ }^{\circ}\text{C}^{-1}$ (Yapp, 1990a) to $0.08\text{‰}\text{ }^{\circ}\text{C}^{-1}$ (Zheng, 1991), to $0.04\text{‰}\text{ }^{\circ}\text{C}^{-1}$ (Clayton and Epstein, 1961). Ongoing experiments, as well as constraints supplied by the isotope chemistry of co-occurring phases, suggest that the fractionations of Zheng (1991) or Clayton and Epstein (1961) are most applicable to Bighorn Basin hematite (Bao *et al.*, 1998). If true, even climatically driven changes in temperature of mineral formation as large as $40\text{ }^{\circ}\text{C}$ would generate shifts in $\delta^{18}\text{O}_{\text{hematite}}$ of only 1.5–3‰. While we cannot presently exclude the possibility that a portion of the signal in $\delta^{18}\text{O}_{\text{hematite}}$ records the effect of temperature change on fractionation, for this discussion we assume that $\delta^{18}\text{O}_{\text{hematite}}$ dominantly records change in the $\delta^{18}\text{O}$ value of surface water.

Thus the record from hematite indicates that the $\delta^{18}\text{O}$ of Bighorn Basin surface water was essentially constant from mid-Clarkforkian through the first 700 ka of the Wasatchian, then dropped rapidly and remained low for over 500 ka before beginning to rise ~ 53.5 Ma. This shift in the isotopic composition of ancient surface water can be related to paleoclimate by assuming that: (1) in this mid-latitude, mid-continental region, variations in the $\delta^{18}\text{O}$ of meteoric water (the ultimate source of surface water) were more strongly correlated to temperature than to amount of precipitation; (2) the slope of the modern relationship between mean annual meteoric water $\delta^{18}\text{O}$ value and MAT can be applied to the Paleogene of North America; and (3) the source of precipitation arriving in the region remained constant throughout the interval. We recognize that these assumptions may be in error. Careful treatment of the meteoric water $\delta^{18}\text{O}$ /MAT relationship for the Paleocene–Eocene transition would require linking oxygen isotope fractionations in atmospheric processes to a climate simulation for the interval. This is beyond the scope of this paper. Instead our goal is to evaluate whether the mid-latitude $\delta^{18}\text{O}$ /MAT slopes of $0.5\text{--}0.6\text{‰}\text{ }^{\circ}\text{C}^{-1}$ observed in the Quaternary (Dansgaard, 1974; Boyle, 1997) supply plausible, consistent estimates of temperature change when applied to the record of change in the $\delta^{18}\text{O}$ of Bighorn Basin surface water. Given these assumptions, the drop in surface water $\delta^{18}\text{O}$ values of 3.25‰ in the earliest Eocene that we infer from $\delta^{18}\text{O}_{\text{hematite}}$ corresponds to a temperature decrease of $5.5\text{--}6.5\text{ }^{\circ}\text{C}$.

No hematite-encrusted bones have been recovered from Wa0 beds, so we cannot evaluate changes in hematite $\delta^{18}\text{O}$ values during the LPTM. However, isotopic records of change in MAT and the $\delta^{18}\text{O}$ of surface water are available for the Bighorn Basin. Koch *et al.* (1995) demonstrated that both soil carbonate and bivalve aragonite from Wa0 beds are enriched in ^{18}O by $\sim 1\text{‰}$ relative to material in underlying Clarkforkian or overlying early Wasatchian sediments. In order to assess changes in MAT from calcite or aragonite, we must consider the effects of temperature both on the $\delta^{18}\text{O}$ of meteoric (and surface) water and on the fractionation of oxygen isotopes between mineral and water. Assuming that the effect of temperature on the fractionation of oxygen isotopes between calcium carbonate and water is

$\sim 0.23\text{‰ }^{\circ}\text{C}^{-1}$ (Friedman and O'Neil, 1977), and that meteoric water $\delta^{18}\text{O}$ increases by a range of $+0.5$ to $0.6\text{‰ }^{\circ}\text{C}^{-1}$ with increases in MAT, an increase in MAT ranging from 2.7 to 3.7°C is required to explain the 1‰ increase in Bighorn Basin soil carbonates and bivalve shells during the LPTM. This would be accomplished by a shift of $+1.6$ to $+1.9\text{‰}$ in the $\delta^{18}\text{O}$ of meteoric and surface water.

CONTINENTAL BIOTIC CHANGE IN THE PALEOCENE-EOCENE TRANSITION

Faunas

The late Paleocene-early Eocene was a period of major mammalian immigration into North America and western Europe. The beginning of the Clarkforkian in North America (during C25n) is recognized by the first appearances of rodents and coryphodontid pantodonts. There are no close relatives of these higher taxa in the earlier Paleocene of North America, implying that they immigrated into North America from another continent. The most significant mammalian immigration event of the Cenozoic occurred at the beginning of the Wasatchian, traditionally recognized as the beginning of the Eocene in continental deposits of North America (Krishtalka *et al.*, 1987). These immigrants also represent orders and families new to North America: primates, even-toed ungulates, odd-toed ungulates, and hyaenodontid creodonts. As at the beginning of the Clarkforkian, the lack of close relatives earlier in the Paleocene implies that these taxa dispersed into North America from another continent. Wasatchian immigrants are known from approximately coeval strata across much of North America, from Mississippi and Baja California in the south to Ellesmere Island in the north (Krishtalka *et al.*, 1987; Beard and Tabrum, 1991). The first appearance of Wasatchian immigrants is approximately synchronous in Europe and North America (Hooker, 1996), strengthening the hypothesis that these taxa dispersed to both continents across high-latitude land bridges. Relatively sketchy knowledge of African and Asian faunas from the Paleocene has made the origins of the Wasatchian immigrants a contentious issue. Recent discoveries in Asia may point to an Asian origin for many of these groups (Beard, 1997). If rodents, coryphodontids, primates, odd-toed and even-toed ungulates, and hyaenodontids all originated in Asia, then the opening of high-latitude land bridges between Asia, North America, and Europe probably had a major effect on the timing of immigration into the latter two continents (Beard, 1997).

The earliest Wasatchian (Wa0) faunas have been identified only in the Bighorn Basin (Gingerich, 1989), where they are contemporaneous with the carbon isotope excursion (Koch *et al.*, 1992, 1995). The Wa0 fauna has the familial composition of typical later Wasatchian assemblages, but many of the species are small compared with earlier and later congeners (Gingerich, 1989; Clyde, 1997). Among living mammals, populations with small body size are associated with warmer climate (Searcy, 1980; Koch, 1986), supporting isotopic evidence for warmer climate during the LPTM. The Wa0 fauna also has the highest species richness and the most equitable distribution of individuals among species of any Paleocene or Eocene faunal interval in the Bighorn Basin sequence (Clyde, 1997), another characteristic of mammalian faunas from areas with warmer climates. The basal Wasatchian

turnover event also modified the trophic structure of the mammalian fauna by increasing the proportion of herbivore/frugivore species (Clyde, 1997). Clyde (1997) has also shown that the taxa immigrating into North America at the beginning of the Wasatchian rapidly became numerically important or dominant members of the mammalian fauna, implying that the faunal transition was ecologically as well as taxonomically significant.

Detailed studies of faunal change during the early Eocene have been confined to the northern Rocky Mountains, therefore the generality of the observations is unknown. Faunal change within the early Eocene is at the generic or specific level. A small pulse of faunal change, called Biohorizon A, has been identified among mammalian faunas from the central Bighorn Basin (Schankler, 1980). Although the existence of Biohorizon A has been attributed to variations in sampling intensity (Badgley and Gingerich, 1988), more recent data tend to confirm the presence of accelerated compositional change at this time (Badgley, 1990; Bown *et al.*, 1994a), which we infer to be about 54.2 Ma. A small number of taxa have last appearances at Biohorizon A (Schankler, 1980, 1981), and three of them reappear synchronously, higher in the Antelope Creek/Elk Creek section near Biohorizon B. Bown *et al.* (1994b) identified several lineages that underwent size increases at Biohorizon A, which is consistent with cooler climates. Faunas from the Foster Gulch/McCullough Peaks section show a small increase in the mean size of individuals in the fauna from Wa2 to Wa3, approximately the same time as Biohorizon A (Clyde, 1997).

A third pulse of mammalian faunal change occurred during the middle of the Wasatchian in the Bighorn Basin, recognized as Biohorizons B and C by Schankler (1980). Bown *et al.* (1994a) argued that Biohorizons B and C were separated by only 40–60 m, and referred to this zone of accelerated turnover as Biohorizon B-C. During this short period, approximately contemporaneous with the beginning of C24n (see discussion above), there are several closely spaced first occurrences (*Bunophorus*, *Heptodon*) and last occurrences (*Haplomylus*, *Ectocion*) of mammalian genera (Bown *et al.*, 1994a). A similar pattern of faunal turnover has been observed in the northern part of the Bighorn Basin (Badgley and Gingerich, 1988; Clyde, 1997). During and just prior to Biohorizon B there was a large increase in morphological variability in many lineages of mammals, followed by a two- to threefold increase in the number of lineages at the species level in the subset of genera that have been studied thoroughly (K. D. Rose, personal communication, 1996). Size decreases in many lineages also occurred in this time interval, which is consistent with renewed climatic warming (Bown *et al.*, 1994b). Size decrease is less noticeable in faunas from the McCullough Peaks area, although the mean individual size for the whole fauna does decrease in the latter part of Wa4, approximately the same as Biohorizon B (Clyde, 1997). Some species-level faunal changes at Biohorizon B may represent *in situ* evolution or intracontinental migration, but intercontinental migration from Asia has been proposed as an explanation for the first appearances of the ungulate genera *Bunophorus* and *Heptodon*, and the slightly later first appearance of *Lambdaotherium* (Beard, 1997).

In summary, there are four intervals of accelerated change in the composition of mammalian faunas during the Paleocene and early Eocene. The beginning

Clarkforkian and beginning Wasatchian events are at a high taxonomic level and probably record northern hemisphere-wide migration across high-latitude land bridges, quite possibly from Asia (Beard, 1997). In the Bighorn Basin the Wasatchian immigration is accompanied by increasing diversity and decreasing body size. These features are consistent with warming climates at middle and high latitudes. The species-level events at Biohorizon A have been observed only in the Bighorn Basin, and may be local, but the body size increases are consistent with paleobotanical and isotopic evidence for cooling in the same sections. The generic-level immigration and body size decrease at Biohorizon B has also been documented best in the Bighorn Basin, and could also be local, but again the changes are consistent with the paleobotanical and isotopic evidence for increasing temperature (Bown *et al.*, 1994b). The last three periods of faunal change are associated with inflections in the temperature curve. The basal Wasatchian immigration coincides with the LPTM (and with the carbon isotope excursion), Biohorizon A coincides with falling temperatures in the early Eocene, and Biohorizon B with rapidly rising temperatures near the beginning of C24n. Later early Eocene faunas are not well represented in the Bighorn Basin, but the transition to Lostcabinian mammalian faunas appears to follow Biohorizon B by less than 500 ka, and takes place during the same rapid warming period.

Floras

Floras of the Paleocene–Eocene interval have been far less studied than mammalian faunas. It has been recognized for some time that Eocene floras of North America have more lineages of modern tropical distribution than do Paleocene floras (e.g., Leopold and MacGinitie, 1972; Wolfe, 1972, 1977; Hickey, 1977). Similarity between the extant warm-temperate floras of North America and East Asia has long been taken as an indication of dispersal across Beringia during the early Cenozoic (e.g., Graham, 1972). Tropical and subtropical taxa shared among Eocene floras of western Europe and North America imply the existence of warm-climate migration corridors across the North Atlantic (Tiffney, 1985a,b). Substantial floral similarity existed between East Asia and North America as early as the late Paleocene (e.g., Brown, 1962; Hickey, 1977; Guo *et al.*, 1984).

Paleocene–Eocene floral change in the Bighorn Basin follows the overall pattern observed elsewhere in the northern hemisphere, but the greater stratigraphic resolution reveals more detail and complexity in the pattern. Change in floral composition is concentrated during two stratigraphic intervals. The first interval begins just following the LPTM (or perhaps during it, since there are no samples from the LPTM interval) and extends through about 30 m of section (approximately 200 ka). The second interval of accelerated change begins between 380 and 420 m in the Antelope Creek/Elk Creek section (near the base of C24n.1), and is completed by 621 m (although it may be shorter because there are almost no plant fossils between 468 and 621 m). This corresponds approximately to the first 600–700 ka of C24n. These intervals of compositional change stand out despite the substantial variability in the floral composition of sites that results from the original heterogeneity in floodplain vegetation and differences in sedimentary environments (Fig. 7.4).

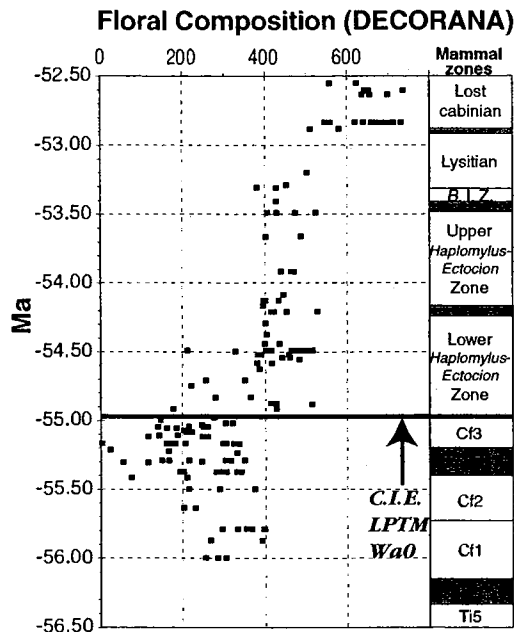


Figure 7.4. Change in floral composition across the Paleocene-Eocene boundary interval. Each point represents one site. Site ages were interpolated using age model 1 (see text). Scores on the x-axis are from the first axis of a detrended correspondence analysis (DECORANA; Hill, 1979) of a site by species matrix of presence/absence data. Abbreviations as in Fig. 7.3.

The first interval of floral turnover is largely the result of last occurrences in the last part of the Clarkforkian and the earliest part of the Wasatchian, combined with the first appearances of several typical Eocene species within 50 m above the Wa0 red beds. Last appearances predominated over first appearances in the late Clarkforkian (Cf3) and throughout the early part of the Wasatchian (50–350 m or 53.5–54.75 Ma), and plant diversity decreased as a consequence (Fig. 7.5). Several of the last occurrences just before the LPTM are of long-ranging Paleocene taxa such as *Ficus artocarpoides* and *Porosia verrucosa*, but many common Paleocene taxa, such as *Eucommia serrata*, *Cornus*, and *Persites argutus*, survived into the early Wasatchian. Although the majority of last appearances near the LPTM are among taxa that have modern relatives that are deciduous and temperate, the number is too small to demonstrate a clear preference in the extinction event.

In the absence of megafossil samples in the Wa0 red beds, it is not possible to tell if floral first occurrences are exactly concurrent with the Wa0 immigration event in mammals, or if they are spread out over a longer time interval. Although marine and terrestrial isotopic records indicate that the LPTM was an interval of rapid warming, the plant taxa making first appearances in the first 20 m above the Wa0 red beds are not thermophiles. Earliest Wasatchian plant immigrants include the deciduous tree *Alnus*, the tree fern *Cnemidaria*, the scrambling fern *Lygodium*,

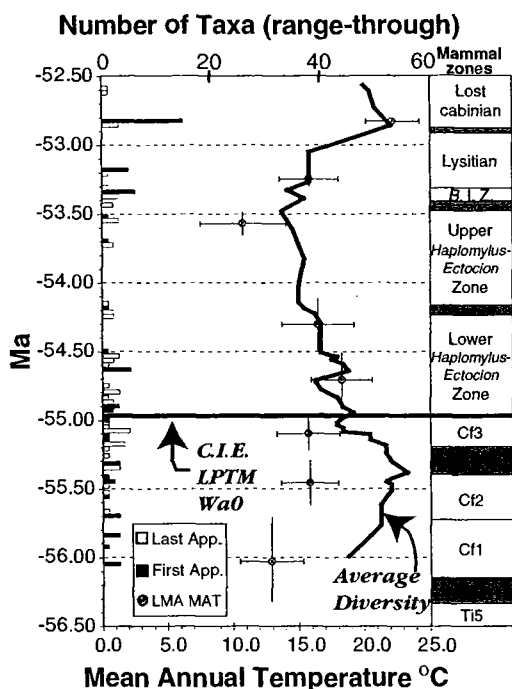


Figure 7.5. Floral richness and turnover across the Paleocene-Eocene boundary interval. Bars indicate the number of first and last occurrences at each stratigraphic level. The line is a two-point running average of the number of species. All calculations were made based on standard range-through assumptions (i.e., taxa were assumed to occur at all levels between their first and last appearance). Abbreviations as in Fig. 7.3.

and the aquatic fern *Salvinia*. *Cnemidaria* and *Salvinia* are today neotropical montane and cosmopolitan subtropical to tropical genera, respectively, but *Alnus* and *Lygodium* are both widely distributed in temperate climates as well as in montane tropical and subtropical areas. If these immigrants share an ecological characteristic, it is the ease with which they are dispersed. The ferns disperse via small, wind-blown spores, and *Alnus* has small, winged seeds that can be carried by wind or water. Although studies of tree migration rates during the Holocene have shown that population movement can potentially be very fast ($100\text{--}500\text{ m year}^{-1}$, Delcourt and Delcourt, 1987), these rates reflect dispersal into recently deglaciated landscape. Tree populations spreading across high-latitude land bridges during the LPTM would presumably have encountered pre-existing forest vegetation, which might have depressed rates of successful establishment following dispersal. This would have greatly reduced migration rates, and might have prevented the spread of all but the most easily dispersed plant species to North America during the 100 ka of the LPTM. Slow rates of plant migration might also explain why there is so much mammalian immigration and so little plant immigration at the base of the Wasatchian.

The second interval of accelerated floral turnover recorded in the Wasatchian is dominated by first occurrences, including many taxa that are ubiquitous in Lostcabinian and early Bridgerian floras in the northern Rocky Mountains. The sharp increase in first occurrences at 621 m (≈ 52.8 Ma) is likely the result of limited sampling in the 200 m below, but the high rates of sediment accumulation in this part of the section imply that the immigration event was rapid, taking place in 500 ka or less (Fig. 7.5). The taxa that appear in the upper part of the Antelope Creek/Elk Creek section tend to have subtropical to tropical distributions today (e.g., Elaeocarpaceae, Apocynaceae, Lauraceae, Myrtaceae, *Machaerium* [Leguminosae]), and the thickness of the compressions and preservation of the cuticle are consistent with their being broad-leaved evergreen trees or shrubs. The influx of new taxa in the interval between 53.3 and 52.8 Ma results in an increase in diversity. Both the diversity increase and the climatic preferences of living relatives of the immigrants are consistent with increasing temperatures at this time in the Bighorn Basin.

As is true with the mammalian fauna, intervals of accelerated floral turnover in the Bighorn Basin appear to correspond to times of more rapid climatic change. The basal Wasatchian plant immigrants are as nearly contemporaneous with the LPTM as sampling allows. The long decline in plant diversity in the early Wasatchian is concurrent with the period of lower temperatures indicated by both isotopic and paleobotanical temperature estimates. The sharp increase in first appearances and in diversity occurs in the same part of the section as the rapid increase in temperature.

Paleobotanical data from outside the Bighorn Basin suggest that the trends described above are at least regional to continental in scope. Changes in floral composition similar to those around the LPTM are seen during the Paleocene–Eocene transition in the Williston Basin of North Dakota (Hickey, 1977), and the increasing floral diversity and change in composition observed in the upper part of the Antelope Creek/Elk Creek section is also observed in association with Lostcabinian mammalian faunas in several parts of southern and central Wyoming (Wing, 1987; Wilf, 1999). The pattern of low latest Paleocene and earliest Eocene diversity followed by rapidly increasing mid–early Eocene diversity is also found in palynofloras from the Gulf Coast of the USA (Frederiksen, 1994). Finally, palynofloras from England also indicate an early Eocene period of lowered diversity (Jolley, 1996). Together these disparate floral data sets provide preliminary evidence that the climatic events associated with late Paleocene and early Eocene floral change in the Bighorn Basin were continental to hemispheric in extent.

CLIMATIC IMPLICATIONS

Two independent lines of evidence confirm the existence of a period of substantial cooling during the early Eocene in the Bighorn Basin, probably beginning ~ 700 ka after the carbon isotope excursion and LPTM, and lasting for approximately the same amount of time. Following this decline, temperatures increased rapidly to their Cenozoic maximum within the first ~ 600 ka after the beginning of C24n. The amplitude of the drop in MAT estimated from leaf margin analysis is

~7.4°C. Oxygen isotope analysis of hematite, which overlaps the early Eocene part of the floral record, corroborates a change in temperature of ~6°C. Between 53.5 and 52.8 Ma, leaf margin estimates indicate an ~10°C increase in MAT. Although oxygen isotopic measurements of hematite are not available for rocks younger than 53 Ma, the initial part of the rise in MAT is accompanied by an ~2‰ increase in the inferred $\delta^{18}\text{O}$ of surface water, consistent with a temperature change of 3.5–4°C.

Because the isotopic and plant-based estimates of MAT come from different sediment, which may represent different parts of short-term climatic cycles and different edaphic conditions on the floodplain, some consistent offset might be expected in temperature estimates from the two different environments. The alternation of oxidized and organic-rich floodplain sediments also dictates that the isotopic and paleobotanical temperature estimates do not represent precisely the same times. All of these factors (different amounts of time averaging, different local conditions, and offsets in the ages of samples) should tend to create differences in MAT records derived from isotopic and paleobotanical sources. Yet both methods indicate an ~700 ka long cool period during the earliest part of the Eocene.

The consistency of floral and oxygen isotope results demonstrates that the observed temperature changes are basin-wide phenomena affecting a range of environments through the region. The thermally driven perturbations in vapor transport that are recorded by the oxygen isotope data are region-to-continental scale features. Furthermore, the faunal and floral events that are coeval with temperature changes in the Bighorn Basin are also known to occur at roughly the same times in other parts of North America. If, as seems likely, the biotic correlates of temperature change are responses rather than coincidences, then the occurrence of the biotic changes over much of North America implies that the climatic driving forces had effects at a continental scope.

Changes in sea level could have caused climatic fluctuations in the late Paleocene and early Eocene of the Bighorn Basin because regressions might be expected to correspond with increased seasonality and colder winter temperatures in continental interiors. During the late Paleocene and early Eocene sea level rose and fell at frequencies roughly similar to those of the temperature changes that we have observed in the Bighorn Basin. The bulk of the Clarkforkian has been correlated to cycle TA 2.1, a time of increasing sea level during the generally high sea levels of the early Paleogene (Haq *et al.*, 1988; Woodburne and Swisher, 1995). A Type 1 sequence boundary (TA 2.1/TA 2.2) during which much of the continental shelf is inferred to have been exposed, has been correlated with the late Clarkforkian (Woodburne and Swisher, 1995). Sea level rose briefly across the Clarkforkian/Wasatchian boundary, but a second Type 1 sequence boundary (TA 2.2/TA 2.3) has been correlated with the earliest Wasatchian (Woodburne and Swisher, 1995). A third Type 1 boundary (TA 2.3/TA 2.4) occurred within the first million years of the Wasatchian, followed by two more minor drops in sea level before the beginning of the Lostcabinian (Woodburne and Swisher, 1995).

Although the Paleocene–Eocene interval is characterized by fairly large transgressive–regressive cycles, the Bighorn Basin temperature records do not show a good temporal correspondence with sea-level change. The TA 2.1/TA 2.2

regression occurs during the warm late Clarkforkian, and the TA 2.2/TA 2.3 regression occurs during the warm earliest Wasatchian. Only the TA 2.3/TA 2.4 regression might correspond to the onset of the cooling we have documented ~ 700 ka following the carbon isotope excursion. The lack of correspondence between sea level and temperature casts doubt on this possible mechanism, although the lack of correspondence could also reflect miscorrelation of marine and continental sequences.

We currently have no good hypotheses to explain early Eocene cooling, but if future observation confirmed this perturbation it considerably complicates the climatic history of the late Paleocene and early Eocene. It appears that over the period from about 58 to 53 Ma, climate in central North America warmed, cooled, then warmed again, with major cooling and warming phases lasting on the order of 1–2 million years. The durations of these fluctuations, whether global or continental in scale, demonstrate climatic variability during a period of early history characterized by globally warm climate and low latitudinal temperature gradients.

CONCLUSIONS

1. High-resolution paleoclimate records can be obtained from continental sections, such as those in the Bighorn Basin, where high sedimentation rates make up for short hiatuses in deposition.
2. Better correlation of continental and marine rocks, based on chemostratigraphy, magnetostratigraphy, and direct dating of strata, will make such records useful in developing a global understanding of paleoclimatic change, as will the use of multiple isotopic and paleontological proxies for climate change.
3. Greater temporal resolution reveals a more complex pattern of climate change than was previously expected, including a substantial cool interval in the early Eocene of the Bighorn Basin.
4. The similarity of floral change through the Paleocene–Eocene transition in different parts of North America suggests that the early Eocene cooling affected at least the whole continent.
5. The causes of cool–warm–cool–warm fluctuation during the late Paleocene and early Eocene are at this point unknown. The fluctuation is too slow to be related to Milankovitch orbital processes, and is not correlated in an obvious way with sea-level changes.
6. The consequences of the cool period show up in patterns of turnover and diversity of terrestrial plants and mammals, and in the body size distribution of the mammals.
7. The duration as well as the magnitude of warming (and cooling?) events may turn out to be an important determinant of their biotic effects.

ACKNOWLEDGEMENTS

We thank Karen Bice and Will Clyde for careful reviews of an earlier draft of this paper, and Jim Zachos and Lisa Sloan for valuable conversations on the stratigraphy and paleoclimate of the Paleocene–Eocene boundary interval. S.L.W. was supported by grants from the Scholarly Studies program of the Smithsonian

Institution and the Evolution of Terrestrial Ecosystems program. P.L.K. was supported by NSF grant EAR 9627953. This is ETE publication no. 65.

REFERENCES

- Ali, J. R. and Hailwood, E. A. (1998). Resolving possible problems associated with magnetostratigraphy of the Paleocene/Eocene boundary in holes 549, 550 (Goban Spur) and 690 B (Maud Rise). *Strata*, **9**, 16–20.
- Aubry, M.-P., Berggren, W. A., Stott, L. and Sinha, A. (1996). The upper Paleocene–lower Eocene stratigraphic record and the Paleocene–Eocene boundary carbon isotope excursion: implications for geochronology. In *Correlation of the Early Paleogene in Northwest Europe*, Geological Society Special Publication No. 101, eds. R. W. O'B. Knox, R. M. Corfield and R. E. Dunay, pp. 353–80. London: Geological Society.
- Badgley, C. (1990). A statistical assessment of last appearances in the Eocene record of mammals. In *Dawn of the Age of Mammals in the Northern Part of the Rocky Mountain Interior, North America*, Geological Society of America Special Paper No. 243, eds. T. M. Bown and K. D. Rose, pp. 153–68. Boulder, CO: Geological Society of America.
- Badgley, C. and Gingerich, P. D. (1988). Sampling and faunal turnover in early Eocene mammals. *Palaeogeography, Paleoclimatology, Palaeoecology*, **63**, 141–57.
- Baker-Brosh, K. F. and Peet, R. K. (1997). The ecological significance of lobed and toothed leaves in temperate forest trees. *Ecology*, **78**, 1250–5.
- Bao, H., Koch, P. L. and Hepple, R. P. (1998). Hematite and calcite coatings on fossil vertebrates. *Journal of Sedimentary Research, A*, **68**, 727–38.
- Beard, K. C. (1997). East of Eden: Asia as an important center of taxonomic origination in mammalian evolution. In *Dawn of the Age of Mammals in Asia*, *Bulletin of the Carnegie Museum of Natural History*, eds. K. C. Beard and M. R. Dawson, **34**, 5–39.
- Beard, K. C. and Tabrum, A. R. (1991). The first early Eocene mammal from eastern North America: an omomyid primate from the Bashi Formation, Lauderdale County, Mississippi. *Mississippi Geology*, **11**, 1–6.
- Becker, R. H. and Clayton, R. N. (1976). Oxygen isotope study of a Precambrian banded iron-formation, Hamersley Range, Western Australia. *Geochimica et Cosmochimica Acta*, **40**, 1153–65.
- Berggren, W. A. and Aubry, M. P. (1996). A late Paleocene–early Eocene NW European and North Sea magnetobiochronological correlation network. In *Correlation of the Early Paleogene in Northwest Europe*, Geological Society Special Publication No. 101, eds. R. W. O'B. Knox, R. M. Corfield and R. E. Dunay, pp. 309–52. London: Geological Society.
- Berggren, W. A., Kent, D. V., Swisher, C. C., III and Aubry, M. P. (1995). A revised Cenozoic geochronology and chronostratigraphy. In *Geochronology, Time Scales and Global Stratigraphic Correlation*, SEPM Special Publication No. 54, eds. W. A. Berggren, D. V. Kent, M. P. Aubry and J. Hardenbol, pp. 129–212. Tulsa, OK: SEPM.
- Bird, M. I., Longstaffe, F. J., Fyfe, W. S. and Bildgen, P. (1992). Oxygen-isotope systematics in a multiphase weathering system in Haiti. *Geochimica et Cosmochimica Acta*, **56**, 2831–8.
- Bird, M. I., Longstaffe, F. J., Fyfe, W. S., Kronberg, B. I. and Kishida, A. (1993). An oxygen-isotope study of weathering in the eastern Amazon Basin, Brazil. In *Climate Change in Continental Isotopic Records*, eds. P. K. Swart *et al.*, *Geophysical Monograph*, **78**, 295–307.

- Bown, T. M. (1979). Geology and mammalian paleontology of the Sand Creek facies, lower Willwood Formation (lower Eocene), Washakie County, Wyoming. *Geological Survey of Wyoming Memoir*, **2**, 1–151.
- Bown, T. M. (1980). Summary of latest Cretaceous and Cenozoic sedimentary, tectonic, and erosional events, Bighorn Basin, Wyoming. In *Early Cenozoic Paleontology and Stratigraphy of the Bighorn Basin, Wyoming*, University of Michigan Papers on Paleontology No. 24, ed. P. D. Gingerich, pp. 25–32. Ann Arbor, MI: University of Michigan.
- Bown, T. M., Holroyd, P. A. and Rose, K. D. (1994b). Mammal extinctions, body size, and paleotemperature. *Proceedings of the National Academy of Science*, **91**, 10403–6.
- Bown, T. M. and Kraus, M. J. (1981a). Lower Eocene alluvial paleosols (Willwood Formation, northwestern Wyoming, USA) and their significance for paleoecology, paleoclimatology, and basin analysis. *Palaeogeography, Palaeoclimatology, Palaeoecology*, **34**, 1–30.
- Bown, T. M. and Kraus, M. J. (1981b). Vertebrate fossil-bearing paleosol units (Willwood Formation, lower Eocene, northwest Wyoming USA: implications for taphonomy, biostratigraphy, and assemblage analysis. *Palaeogeography, Palaeoclimatology, Palaeoecology*, **34**, 31–56.
- Bown, T. M. and Kraus, M. J. (1993). Time-stratigraphic reconstruction and integration of paleopedologic, sedimentologic, and biotic events (Willwood Formation, lower Eocene, northwest Wyoming, USA). *Palaios*, **8**, 68–80.
- Bown, T. M., Rose, K. D., Simons, E. L. and Wing, S. L. (1994a). Distribution and stratigraphic correlation of upper Paleocene and lower Eocene fossil mammal and plant localities of the Fort Union, Willwood, and Tatman Formations, southern Bighorn Basin, Wyoming. *US Geological Survey Professional Paper*, **1540**, 1–269.
- Boyle, E. A. (1997). Cool tropical temperatures shift the global $\delta^{18}\text{O}$ -T relationship: an explanation for the ice core $\delta^{18}\text{O}$ -borehole thermometry conflict? *Geophysical Research Letters*, **24**, 273–6.
- Brown, R. W. (1962). Paleocene flora of the Rocky Mountains and Great Plains. *US Geological Survey Professional Paper*, **375**, 1–119.
- Budantsev, L. Y. (1992). Early stages of formation and dispersal of the temperate flora in the Boreal region. *The Botanical Review*, **58**, 1–48.
- Butler, R. F., Gingerich, P. D. and Lindsay, E. H. (1981). Magnetic polarity stratigraphy and biostratigraphy of Paleocene and lower Eocene continental deposits, Clark's Fork Basin, Wyoming. *Journal of Geology*, **89**, 299–316.
- Cande, S. C. and Kent, D. V. (1992). A new geomagnetic polarity time scale for the Late Cretaceous and Cenozoic. *Journal of Geophysical Research*, **97**, 13917–51.
- Cande, S. C. and Kent, D. V. (1995). Revised calibration of the geomagnetic polarity time scale for the Late Cretaceous and Cenozoic. *Journal of Geophysical Research*, **100**, 6093–5.
- Canny, M. J. (1990). What becomes of the transpiration stream? *New Phytologist*, **114**, 341–68.
- Cerling, T. E. and Quade, J. (1993). Stable carbon and oxygen isotope in soil carbonates. In *Climate Change in Continental Isotopic Records*, eds. P. K. Swart *et al.*, *Geophysical Monograph*, **78**, 217–31.
- Christophel, D. C. and Greenwood, D. R. (1989). Changes in climate and vegetation in Australia during the Tertiary. *Review of Palaeobotany and Palynology*, **58**, 95–109.
- Clayton, R. N. and Epstein, S. (1961). The use of oxygen isotopes in high temperature geological thermometry. *Journal of Geology*, **69**, 447–52.
- Clyde, W. C. (1997). *Stratigraphy and Mammalian Paleontology of the McCullough Peaks, Northern Bighorn Basin, Wyoming: Implications for Biochronology*. Basin

- Development, and Community Reorganization across the Paleocene–Eocene Boundary.* PhD thesis, Department of Geology, University of Michigan, Ann Arbor, MI.
- Clyde, W. C., Stamatakos, J. and Gingerich, P. D. (1994). Chronology of the Wasatchian land-mammal age (early Eocene): magnetostratigraphic results from the McCullough Peaks section, northern Bighorn Basin, Wyoming. *Journal of Geology*, **102**, 367–77.
- Collinson, M. E. and Hooker, J. J. (1987). Vegetational and mammalian faunal changes in the Early Tertiary of southern England. In *The Origins of Angiosperms and their Biological Consequences*, eds. E. M. Friis, W. G. Chaloner and P. R. Crane, pp. 259–304. New York: Cambridge University Press.
- Corfield, R. M. and Norris, R. D. (1996). Deep water circulation in the Paleocene Ocean. In *Correlation of the Early Paleogene in Northwest Europe*, Geological Society Special Publication No. 101, eds. R. W. O'B. Knox, R. M. Corfield and R. E. Dunay, pp. 443–56. London: Geological Society.
- Dansgaard, W. (1964). Stable isotopes in precipitation. *Tellus*, **16**, 436–68.
- Davies-Vollum, S. K. and Wing, S. L. (1998). Sedimentological, taphonomic, and climatic aspects of Eocene swamp deposits (Willwood Formation, Bighorn Basin, Wyoming). *Palaos*, **13**, 28–40.
- Delcourt, P. A. and Delcourt, H. R. (1987). *Long-Term Forest Dynamics of the Temperate Zone*. New York: Springer-Verlag.
- Dickens, G. R., Castillo, M. M. and Walker, J. C. G. (1997). A blast of gas in the latest Paleocene: simulating first-order effects of massive dissociation of oceanic methane hydrate. *Geology*, **25**, p. 259–62.
- Frederiksen, N. O. (1979). Paleogene sporomorph biostratigraphy, northeastern Virginia. *Palynology*, **3**, 129–67.
- Frederiksen, N. O. (1980). Paleogene sporomorphs from South Carolina and quantitative correlations with the Gulf Coast. *Palynology*, **4**, 125–79.
- Frederiksen, N. O. (1994). Paleocene floral diversities and turnover events in eastern North America and their relation to diversity models. *Review of Palaeobotany and Palynology*, **82**, 225–38.
- Friedman, I. and O'Neil, J. R. (1977). Compilation of stable isotope fractionation factors of geochemical interest. *US Geological Survey Professional Paper*, **440**, 1–12.
- Gibson, T. G., Bybell, L. M. and Owens, J. P. (1993). Latest Paleocene lithologic and biotic events in neritic deposits of southwestern New Jersey. *Paleoceanography*, **8**, 495–514.
- Gingerich, P. D., (1983). Paleocene–Eocene faunal zones and a preliminary analysis of Laramide structural deformation in the Clark's Fork Basin, Wyoming. *Wyoming Geological Association Annual Field Conference Guidebook*. **34**, 185–95.
- Gingerich, P. D. (1989). New earliest Wasatchian mammalian fauna from the Eocene of northwestern Wyoming: Composition and diversity in a rarely sampled high-flood-plain assemblage. *University of Michigan Papers on Paleontology*, **28**, 1–97.
- Gingerich, P. D. (1991). Systematics and evolution of Early Eocene Perissodactyla (Mammalia) in the Clarks Fork Basin, Wyoming. *Contribution from the Museum of Paleontology, University of Michigan*, **28**, 181–213.
- Gingerich, P. D., Rose, K. D. and Krause, D. W. (1980). Cenozoic mammalian faunas of the Clark's Fork Basin–Polecat Bench area, northwestern Wyoming. In *Early Cenozoic Paleontology and Stratigraphy of the Bighorn Basin, Wyoming*, University of Michigan Papers on Paleontology No. 24, ed. P. D. Gingerich, pp. 51–64. Ann Arbor, MI: University of Michigan.
- Givnish, T. J. (1979). On the adaptive significance of leaf form. In *Topics in Plant Population Biology*, eds. O. T. Solbrig, S. Jain, G. B. Johnson and P. H. Raven, pp. 375–407. New York: Columbia University Press.

- Graham, A. (1972). Outline of the origin and historical recognition of floristic affinities between Asia and eastern North America. In *Floristics and Paleofloristics of Asia and Eastern North America*, ed. A. Graham, pp. 1–18. Amsterdam: Elsevier.
- Graham, A. (1992). Neotropical Paleogene coastal floras $^{18}\text{O}/^{16}\text{O}$ -estimated warmer vs. cooler equatorial waters. *American Journal of Botany*, **79** (supplement), 102.
- Greenwood, D. R. (1992). Taphonomic constraints on foliar physiognomic interpretations of Late Cretaceous and Tertiary palaeoclimates. *Review of Palaeobotany and Palynology*, **71**, 149–90.
- Guo, S-X. (1985). Preliminary interpretation of Tertiary climate by using megafossil floras in China. *Palaeontologia Cathayana*, **2**, 169–75.
- Guo, S-X., Sun, Z-H., Li, H-M. and Dou, Y-W. (1984). Paleocene megafossil flora from Altai of Xinjiang. *Bulletin of Nanjing Institute of Geology and Palaeontology, Academia Sinica*, **8**, 119–46.
- Haq, B. U., Hardenbol, J. and Vail, P. R. (1988). Mesozoic and Cenozoic chronostratigraphy and cycles of sea-level change. In *Sea-Level Changes: An Integrated Approach*, SEPM Special Publication No. 42, eds. C. K. Wilgus, B. S. Hastings, C. A. Ross, H. Posamentier, J. Van Wagoner and C. G. St. C. Kendall, pp. 71–108. Tulsa, OK: SEPM.
- Hickey, L. J. (1977). Stratigraphy and paleobotany of the Golden Valley Formation (early Tertiary) of western North Dakota. *Geological Society of America Memoir*, **150**, 1–181.
- Hickey, L. J. (1980). Paleocene stratigraphy and flora of the Clark's Fork Basin. In *Early Cenozoic Paleontology and Stratigraphy of the Bighorn Basin, Wyoming*, University of Michigan Papers on Paleontology No. 24, ed. P. D. Gingerich, pp. 33–49. Ann Arbor, MI: University of Michigan.
- Hickey, L.J. and Wolfe, J.A. (1975). The bases of angiosperm phylogeny: vegetative morphology. *Annals of the Missouri Botanical Garden*, **62**, 538–89.
- Hill, M. O. (1979). *DECORANA, a FORTRAN program for Detrended Correspondence Analysis and Reciprocal Averaging*. Ithaca, New York: Microcomputer Power.
- Hooker, J. J. (1996). Mammalian biostratigraphy across the Paleocene–Eocene boundary in the Paris, London and Belgian basins. In *Correlation of the Early Paleogene in Northwest Europe*, Geological Society Special Publication No. 101, eds. R. W. O'B. Knox, R. M. Corfield and R. E. Dunay, pp. 205–18. London: Geological Society.
- Hutchison, J. H. (1982). Turtle, crocodylian, and champsosaur diversity changes in the Cenozoic of the north-central region of western United States. *Palaeogeography, Palaeoclimatology, Palaeoecology*, **37**, 149–64.
- Johnston, J. H. and Lewis, D. G. (1983). A detailed study of the transformation of ferrihydrite to hematite in an aqueous medium at 92°C. *Geochimica et Cosmochimica Acta*, **47**, 1823–31.
- Jolley, D. W. (1996). The earliest Eocene sediments of eastern England: and ultra-high resolution palynological correlation. In *Correlation of the Early Paleogene in Northwest Europe*, Geological Society Special Publication No. 101, eds. R. W. O'B. Knox, R. M. Corfield and R. E. Dunay, pp. 219–54. London: Geological Society.
- Kennett, J. P. and Stott, L. D. (1991). Abrupt deep-sea warming, palaeoceanographic changes and benthic extinctions at the end of the Palaeocene. *Nature*, **353**, 225–9.
- Koch, P. L. (1986). Clinal geographic variation in mammals: implications for the study of chronoclines. *Paleobiology*, **12**, 269–81.
- Koch, P. L., Zachos, J. C. and Dettmann, D. L. (1995). Stable isotope stratigraphy and paleoclimatology of the Paleogene Bighorn Basin (Wyoming, U.S.A.). *Palaeogeography, Palaeoclimatology, Palaeoecology*, **115**, 61–89.

- Koch, P. L., Zachos, J. C. and Gingerich, P. D. (1992). Correlation between isotope records in marine and continental carbon reservoirs near the Palaeocene/Eocene boundary. *Nature*, **358**, 319–22.
- Kraus, M. J. and Aslan, A. (1993). Eocene hydromorphic paleosols: significance for interpreting ancient floodplain processes. *Journal of Sedimentary Petrology*, **63**, 453–63.
- Kraus, M. J. and Bown, T. M. (1993). Short-term sediment accumulation rates determined from Eocene alluvial paleosols. *Geology*, **21**, 743–6.
- Krishtalka, L., West, R. M., Black, C. C. *et al.* (1987). Eocene (Wasatchian through Duchesnean) biochronology of North America. In *Cenozoic Mammals of North America Geochronology and Biostratigraphy*, ed. M. O. Woodburne, pp. 77–117. Berkeley, CA: University of California Press.
- Lawrence, J. R. and Taylor, H. P. Jr. (1972). Hydrogen and oxygen isotope systematics in weathering profiles. *Geochimica et Cosmochimica Acta*, **36**, 1377–93.
- Leopold, E. B. and MacGinitie, H. D. (1972). Development and affinities of Tertiary floras in the Rocky Mountains. In *Floristics and Paleofloristics of Asia and Eastern North America*, ed. A. Graham, pp. 147–200. Amsterdam: Elsevier.
- MacGinitie, H. D. (1969). The Eocene Green River flora of northwestern Colorado and northeastern Utah. *University of California Publications in Geological Sciences*, **83**, 1–202.
- Markwick, P. J. (1994). 'Equability,' continentality and Tertiary 'climate': the crocodylian perspective. *Geology*, **22**, 613–6.
- McKeague, J. A., Cheshire, M. V., Andreux, F. and Berthelin, J. (1986). Organo-mineral complexes in relation to pedogenesis. In *Interactions of Soil Minerals with Natural Organics and Microbes*, Soil Science Society of America Special Publication No. 17, eds. P. M. Huang and M. Schnitzer, pp. 549–92. Madison, WI: Soil Science Society of America.
- Miller, K. G., Fairbanks, R. G. and Mountain, G. S. (1987). Tertiary oxygen isotope synthesis, sea level history, and continental margin erosion. *Paleoceanography*, **2**, 1–19.
- Quade, J., Cerling, T. E. and Bowman, J. R. (1989). Systematic variation in the carbon and oxygen isotopic composition of pedogenic carbonate along elevation transects in the southern Great Basin, United States. *Geological Society of America Bulletin*, **101**, 464–75.
- Robert, C. and Kennett, J. P. (1994). Antarctic subtropical humid episode at the Paleocene–Eocene boundary: clay-mineral evidence. *Geology*, **22**, 211–4.
- Romero, E. J. (1986). Paleogene phytogeography and paleoclimatology of South America. *Annals of the Missouri Botanical Garden*, **73**, 449–61.
- Rose, K. D. (1981). The Clarkforkian land-mammal age and mammalian faunal composition across the Paleocene–Eocene boundary. *University of Michigan Papers on Paleontology*, **26**, 1–197.
- Rozanski, K., Araguas-Araguas, L. and Gonfiantini, R. (1993). Isotopic patterns in modern global precipitation. In *Climate Change in Continental Isotopic Records*, eds. P. K. Swart *et al.*, *Geophysical Monograph*, **78**, 1–36.
- Savin, S. M. and Epstein, S. (1970). The oxygen and hydrogen isotope geochemistry of clay minerals. *Geochimica et Cosmochimica Acta*, **34**, 25–42.
- Schankler, D. M. (1980). Faunal zonation of the Willwood Formation in the central Bighorn Basin, Wyoming. In *Early Cenozoic Paleontology and Stratigraphy of the Bighorn Basin, Wyoming*, University of Michigan Papers on Paleontology No. 24, ed. P. D. Gingerich, pp. 99–114. Ann Arbor, MI: University of Michigan.
- Schankler, D. M. (1981). Local extinction and ecological re-entry of early Eocene mammals. *Nature*, **293**, 135–8.

- Schrag, D., DePaolo, D. J. and Richter, F. M. (1992). Oxygen isotope exchange in a two-layer model of oceanic crust. *Earth and Planetary Science Letters*, **111**, 305–17.
- Schwertmann, U. and Murad, E. (1983). Effect of pH on the formation of goethite and hematite from ferrihydrite. *Clays and Clay Minerals*, **31**, 277–84.
- Schwertmann, U. and Taylor, R. M. (1989). Iron oxides. In *Minerals in Soil Environments*, SSSA Book Series 1, eds. J. B. Dixon and S. B. Weed, pp. 379–438. Madison, WI: Soil Science Society of America.
- Searcy, W. A. (1980). Optimum body sizes at different temperatures: an energetics explanation of Bergmann's rule. *Journal of Theoretical Biology*, **83**, 579–93.
- Swisher, C. C., III and Knox, R. W. O'B. (1991). The age of the Paleocene/Eocene boundary: $^{40}\text{Ar}/^{39}\text{Ar}$ dating of the lower part of NP10, North Sea Basin and Denmark. In *IGCP Project 308 (Paleocene/Eocene boundary events)*, International Annual Meeting and Field Conference, Brussels, 2–6 December 1991, Abstracts with Program, p. 16.
- Tauxe, L., Gee, J., Gallet, Y., Pick, T. and Bown, T. M. (1994). Magnetostratigraphy of the Willwood Formation, Bighorn Basin, Wyoming: new constraints on the location of the Paleocene/Eocene boundary. *Earth and Planetary Science Letters*, **125**, 159–72.
- Tiffney, B. H. (1985a). Perspectives on the origin of the floristic similarity between eastern Asia and eastern North America. *Journal of the Arnold Arboretum*, **66**, 73–94.
- Tiffney, B. H. (1985b). The Eocene North Atlantic land bridge: its importance in Tertiary and modern phytogeography of the northern hemisphere. *Journal of the Arnold Arboretum*, **66**, 243–73.
- Valley, J. W., Kitchen, N., Kohn, M. J., Niendorf, C. R. and Spicuzza, M. J. (1995). UWG-2, a garnet standard for oxygen isotope ratios: strategies for high precision and accuracy with laser heating. *Geochimica et Cosmochimica Acta*, **59**, 5223–31.
- Wilf, P. (1997). When are leaves good thermometers? A new case for Leaf Margin Analysis. *Paleobiology*, **23**, 373–90.
- Wilf, P. D. (1999). Paleobotanical analysis of late Paleocene–early Eocene climate changes in the greater Green River Basin of southwestern Wyoming. *GSA Bulletin* (in press).
- Wing, S. L. (1984). A new basis for recognizing the Paleocene/Eocene boundary in western interior North America. *Science*, **226**, 439–41.
- Wing, S. L. (1987). Eocene and Oligocene floras and vegetation of the northern Rocky Mountains. *Annals of the Missouri Botanical Garden*, **74**, 748–84.
- Wing, S. L. (1998). Late Paleocene–early Eocene floral and climatic change in the Bighorn Basin, Wyoming. In *Late Paleocene–Early Eocene Biotic and Climatic Events*, eds. W. Berggren, M. P. Aubry and S. Lucas. New York: Columbia University Press.
- Wing, S. L., Alroy, J. and Hickey, L. J. (1995). Plant and mammal diversity in the Paleocene to early Eocene of the Bighorn Basin. *Palaeogeography, Palaeoclimatology, Palaeoecology*, **115**, 117–56.
- Wing, S. L. and Bown, T. M. (1985). Fine scale reconstruction of late Paleocene–early Eocene paleogeography in the Bighorn Basin of northern Wyoming. In *Cenozoic Paleogeography of West-Central United States*, eds. R. M. Flores and S. S. Kaplan, pp. 93–105. Denver, CO: SEPM, Rocky Mountain Section.
- Wing, S. L., Bown, T. M. and Obradovich, J. D. (1991). Early Eocene biotic and climatic change in interior western North America. *Geology*, **19**, 1189–92.
- Wing, S. L. and Greenwood, D. R. (1993). Fossils and fossil climate: the case for equable continental interiors in the Eocene. In *Palaeoclimates and their Modeling with Special Reference to the Mesozoic Era*, eds. J. R. L. Allen, B. J. Hoskins, B. W. Sellwood and R. A. Spicer. *Philosophical Transactions of the Royal Society, London B, Biological Sciences*, **341**, 243–52.

- Winograd, I. J., Coplen, T. B., Landwehr, J. M. *et al.* (1992). Continuous 500,000-year climate record from vein calcite in Devils Hole, Nevada. *Science*, **258**, 255–60.
- Wolfe, J. A. (1966). Tertiary plants from the Cook Inlet Region, Alaska. *US Geological Survey Professional Paper*, **398-B**, 1–32.
- Wolfe, J. A. (1972). An interpretation of Alaskan Tertiary floras. In *Floristics and Paleofloristics of Asian and Eastern North America*, ed. A. Graham, pp. 201–33. Amsterdam: Elsevier.
- Wolfe, J. A. (1977). Paleogene floras from the Gulf of Alaska region. *US Geological Survey Professional Paper*, **997**, 1–108.
- Wolfe, J. A. (1979). Temperature parameters of humid to mesic forests of eastern Asia and relation to forests of other regions of the northern hemisphere and Australasia. *US Geological Survey Professional Paper*, **1106**, 1–37.
- Wolfe, J. A. (1993). A method of obtaining climatic parameters from leaf assemblages. *US Geological Survey Bulletin*, **2040**, 1–71.
- Woodburne, M. O. and Swisher, C. C. (1995). Land mammal high-resolution geochronology, intercontinental overland dispersals, sea level, climate, and vicariance. In *Geochronology, Time Scales and Global Stratigraphic Correlation*, SEPM Special Publication No. 54, eds. W. A. Berggren, D. V. Kent, M. P. Aubry and J. Hardenbol, pp. 335–64. Tulsa, OK: SEPM.
- Yapp, C. J. (1987). Oxygen and hydrogen isotope variations among goethites (α -FeOOH) and the determination of paleotemperatures. *Geochimica et Cosmochimica Acta*, **51**, 355–64.
- Yapp, C. J. (1990a). Oxygen isotopes in iron (III) oxides: 1, mineral-water fractionation factors. *Chemical Geology*, **85**, 329–35.
- Yapp, C. J. (1990b). Oxygen isotope effects associated with the solid-state α -FeOOH to α -Fe₂O₃ phase transformation. *Geochimica et Cosmochimica Acta*, **54**, 229–36.
- Yapp, C. J. (1991). Oxygen isotopes in an oolitic ironstone and the determination of goethite $\delta^{18}\text{O}$ values by selective dissolution of impurities: The 5 M NaOH method. *Geochimica et Cosmochimica Acta*, **55**, 2627–34.
- Yapp, C. J. (1993). The stable isotope geochemistry of low temperature Fe(III) and Al “oxides” with implications for continental paleoclimates. In *Climate Change in Continental Isotopic Records*, eds. P. K. Swart *et al.*, *Geophysical Monograph*, **78**, 285–94.
- Yapp, C. J. (1997). An assessment of isotopic equilibrium in goethites from a bog iron and a lateritic regolith. *Chemical Geology*, **135**, 159–71.
- Zachos, J. C., Stott, L. D. and Lohmann, K. C. (1994). Evolution of early Cenozoic marine temperatures. *Paleoceanography*, **9**, 353–87.
- Zheng, Y.-F. (1991). Calculation of oxygen isotope fractionation in metal oxides. *Geochimica et Cosmochimica Acta*, **55**, 2299–307.

